Developmental Biology 377 (2013) 138–153

Contents lists available at SciVerse ScienceDirect

Developmental Biology

journal homepage: www.elsevier.com/locate/developmentalbiology

Activation and function of TGFβ signalling during Drosophila wing development and its interactions with the BMP pathway

Covadonga F. Hevia, Jose F. de Celis *

Centro de Biología Molecular "Severo Ochoa", CSIC and Universidad Autónoma de Madrid, Madrid 28049, Spain

ARTICLE INFO

Article history:
Received 10 October 2012
Received in revised form
26 December 2012
Accepted 6 February 2013
Available online 26 February 2013

Keywords:
Smad2
Mad
Signalling
RNA interference
TGFβ ligands

ABSTRACT

The development of the Drosophila wing disc requires the activities of the BMP and TGFβ signalling pathways. BMP signalling is critical for the correct growth and patterning of the disc, whereas the related TGFβ pathway is mostly required for growth. The BMP and TGFβ pathways share a common co-receptor (Punt) and a nuclear effector (Medea), and consequently it is likely that these pathways can interfere with each other during normal development. In this work we focus on the spatial activation domains and requirements for TGFβ signalling during wing disc development. We found that the phosphorylation of Smad2, the specific transducer for TGFβ signalling, occurs in a generalised manner in the wing disc. It appears that the expression of the four candidate TGFβ ligands (Activinβ, Dawdle, Maverick and Myoglianin) in the wing disc is required to obtain normal levels of TGFβ signalling in this tissue. We show that Baboon, the specific receptor of the TGFβ pathway, can phosphorylate Mad, the specific transducer of the BMP pathway, in vivo. However, this activation only occurs in the wing disc when the receptor is constitutively activated in a background of reduced expression of Smad2. In the presence of Smad2, the normal situation during wing disc development, high levels of activated Baboon lead to a depletion in Mad phosphorylation and to BMP loss-of-function phenotypes. Although loss of either *babo* or *Smad2* expression reduce growth in the wing blade in a similar manner, loss of *Smad2* can also cause phenotypes related to ectopic BMP signalling, suggesting a physiological role for this transducer in the regulation of Mad spatial activation.

Introduction

Transforming growth factor-beta/Activin (TGFβ) and bone morphogenetic protein (BMP) signalling pathways are related and conserved modules that participate in a variety of key biological processes including stem cell development, cell proliferation, migration, differentiation and apoptosis (Massague et al., 2000; Schmierer and Hill, 2007; Huang and Chen, 2012). The biochemical structure of the TGFβ and BMP pathways is known, and the ligands, receptors and transducers of each pathway are well conserved during evolution. In summary, ligands of the TGFβ and BMP families activate a complex of type I and type II transmembrane receptors with Serine/Threonine kinase activity which in turn phosphorylates effectors named Smads. Activated Smad complexes translocate to the nucleus and, in conjunction with other transcription factors, regulate the expression of downstream genes (Massague and Wotton, 2000; Wu and Hill, 2009). The main distinction between the TGFβ and BMP pathways lies in the ligands, the particular receptor complex bound by the ligands and the identity of the Smad proteins that these receptors phosphorylate (Schmierer and Hill, 2007). Receptor activation involves the phosphorylation of serines and threonines in the GS domain of a type I receptor by a type II receptor. Type I receptors are specific for TGFβ or BMP ligands, whereas type II receptors are common for both ligand families (Massague et al., 2000; Schmierer and Hill, 2007; Huang and Chen, 2012). Once activated, the type I receptor recruits and phosphorylates a specific receptor-regulated Smad (R-Smad), which form heterodimers with a common co-regulated Smad (co-Smad) and translocates to the nucleus (Massague et al., 2005; Wu and Hill, 2009). In Drosophila, the type I receptor for TGFβ ligands is Baboon (*babo*), the main type I receptor for BMP ligands is Thickveins (*tkv*), and the common type II receptor for both pathways is Punt (*put*) (Parker et al., 2004). The Smad family in Drosophila is formed by dSmad2 (*Smox*), involved in TGFβ signalling and related to vertebrate Smad2 and 3; Mad, that participates in the BMP pathway and is related to Smad1 and 5, and Med, the co-Smad for the TGFβ and BMP pathways orthologous of vertebrate Smad4 (Parker et al., 2004; Raftery and Sutherland, 1999).

The BMP pathway participates in many aspects of Drosophila embryonic and imaginal development (Affolter et al., 1994; Raftery and Sutherland, 1999). In the wing imaginal disc, the epithelial

* Corresponding author. Fax: +34 911964698.
E-mail address: jfdecelis@cbm.uam.es (J.F. de Celis).

0012-1606/$ - see front matter © 2013 Elsevier Inc. All rights reserved.
http://dx.doi.org/10.1016/j.ydbio.2013.02.004

structure that gives rise to the wing and thorax of the fly, the ligand Decapentaplegic (*dpp*) is expressed in a stripe of anterior cells abutting the antero-posterior compartment boundary, and signalling by the Tkv/Put receptor complex and Mad/Med heterodimers is required for the growth and patterning of the wing disc and for the differentiation of the wing veins (Posakony et al., 1990; Burke and Basler, 1996; Sanicola et al., 1995). Most emphasis in the analysis of the TGFβ pathway concerns its activity during neural development and physiology. In this system, TGFβ signalling is required for the proliferation of neuroblasts, to generate an appropriate number of neuronal cells in the central nervous system, and it is also extensively used for axonal remodelling, participating in the establishment of functional connections between the neurons and its targets (Parker et al., 2006; Ting et al., 2007; Zheng et al., 2003, 2006; Zhu et al., 2008). The TGFβ pathway also contributes to imaginal development, where signalling by Babo/Put is required for the growth of the discs (Brummel et al., 1999; Das et al., 1999). In this system, most evidence suggests independent requirements of BMP/Tkv/Mad and TGFβ/Babo/Smad2. Thus, *babo* function does not contribute to the regulation of Tkv/Put target genes, and *babo* mutants do not affect the formation of the veins (Brummel et al., 1999). Some data, however, lead to the suggestion that the main role of Smad2 in the wing disc is to inhibit the response of wing intervein cells to BMP/Tkv/Mad signalling (Sander et al., 2010), an effect not found for the receptor Babo. Furthermore, it has been shown that Actβ, Daw and Babo expressed in cultured cells can also activate Mad, the BMP-specific Smad, adding further complexity to the relationships between the receptors and their downstream Smads (Gesualdi and Haerry, 2007). Similar caveats exist as to the nature and mode of action of the candidate TGFβ ligands in the wing disc. For example, it appears that among the four TGFβ ligands present in the Drosophila genome, only Actβ reproduces the effects of the expression of activated forms of Babo in promoting extra-growth of the wing (Gesualdi and Haerry, 2007). As Actβ expression has not been detected in imaginal discs, it was been suggested that Actβ expressed in the central neural system regulates wing growth through Babo by paracrine signalling (Gesualdi and Haerry, 2007).

In this work, we study the requirement and pattern of activation of TFGβ signalling during wing disc development, the expression and function of the TFGβ ligands in the wing disc and the interactions between the Tkv/Put/Mad and Babo/Put/Smad2 signalling systems. We found that Smad2 is required to promote imaginal disc growth downstream of Babo, and that the pattern of activation of the pathway is generalised in the wing disc epithelium. Babo/Smad2 activity does not regulate any specific step of the cell cycle, but influences cell division rates and cell growth. We detected expression of the four genes encoding members of the TGFβ superfamily in the wing disc. These genes, *dActivinβ* (*actβ*), *dawdle* (*daw*), *maverick* (*mav*) and *myoglianin* (*myo*), are expressed in a generalised manner in this tissue, and in more restricted patterns in other imaginal discs and in the larval brain. Furthermore, knockdown of each gene in the wing disc results in modest phenotypes of wing size reduction without affecting the pattern of veins, suggesting that all of them contribute to Smad2 activation. Finally, we identify that expression of a constitutively activated form of Babo in wing imaginal cells induces Smad2 activation and, simultaneously, strongly reduces Mad phosphorylation. Most revealing, the effects of activated Babo on Mad are reversed when activated Babo is expressed in the absence of Smad2. In this context, activated Babo promotes with high efficiency the phosphorylation of Mad. Loss of endogenous *babo* does not interfere with Mad phosphorylation, suggesting that Babo does not influence the signalling outcome of BMP signalling during normal wing disc development. However, loss of Smad2, in addition to defective growth of the wing pouch, leads to an expansion of the lateral regions of the wing disc and to weak extra-vein phenotypes, suggesting that the presence of Smad2 can limit BMP/Mad signalling. We suggests that competitive interactions between components of the BMP and TGFβ pathways might be critical to determine the outcome of signalling in particular developmental contexts or in pathological conditions caused by mutations in BMP/TGFβ components.

Material and methods

Drosophila genetic strains

We used the Gal4 lines 638-*Gal*4, *nub-Gal*4, *hh-Gal*4, *en-Gal*4 and sal^{EPv}-*Gal*4 (Cruz et al., 2009) and *da-Gal*4. 638-*Gal*4 is an insertion of P-Gal4 in the 5′ region of the *scalloped* gene (not shown). The expression of 638-*Gal*4 and *nub-Gal*4 is restricted to the wing blade or wing blade plus hinge, respectively in third instar wing discs (Supplementary Fig. 1). The expression of *hh-Gal*4 and *en-Gal*4 is restricted to the posterior compartment of all imaginal discs, the expression of sal^{EPv}-*Gal*4 is limited to a central domain of the wing blade and the expression of *da-Gal*4 is ubiquitous in larvae (Supplementary Fig. 1 and data not shown). We used the UAS-lines *UAS-GFP*, UAS-CD8-GFP, $UAS\text{-}babo^{QD}$ (babo*), $UAS\text{-}tkv^{QD}$ (tkv*), $UAS\text{-}Mad^{SDVD}$ (Mad*), $UAS\text{-}Smad^{SDVD}$ (Smad2*), *UAS-dpp-GFP*, *UAS-babo*, *UAS-put*, (Gesualdi and Haerry, 2007; Nellen et al., 1996; Teleman and Cohen, 2000), the Smad2 reporter line $Smox^{G0348}$ and the alleles $babo^{32}$, *P{lacW}-*$babo^{k16912}$ and put^{135}. We also used the following UAS lines to express RNA interference: *UAS-Smad2-i* (2262R-1, NIG-FLY; 105687KK, VDCR and 26756, BDSC), *UAS-babo-i* (8224R-3, NIG-FLY, 106092KK and 3825GD, VDCR and 25933, BDSC), *UAS-tkv-i* (862; VDRC), *UAS-put-i* (7904R-2, NIG-FLY), *UAS-Mad-i* (12399R-2 NIG-FLY), *UAS-Med-i* (19688; VDRC), *UAS-daw-i* (105309KK, VDRC; 16987R-2, NIG-FLY and 34974, BDSC), *UAS-actβ-ι* (108663KK and 12174GD, VDCR and 11062R-1, NIG-FLY), *UAS-mav-i* (1901R-3 and 1901R-3, NIG-FLY and 36809, BDSC), and *UAS-myo-i* (33132GD, VDCR; 1838R1 and 1838R-3, NIG-FLY and 36840, BDSC). Unless otherwise stated, crosses were done at 25 °C. Lines not described in the text can be found in FlyBase (Drysdale, 2008).

Clonal analysis

Clones were generated by FLP induced mitotic recombination in larvae of the following genotypes:

- *hsFLP*1.22; *FRT42D P{UbiGFP}*/*FRT42D* $babo^{32}$
- *hsFLP*1.22; *FRT42D P{UbiGFP}*/*FRT42D* $babo^{k16912}$
- *hsFLP*1.22; *act-FRT < STOP > FRT-lacZ*/+; *UAS-Smad2-i*/*hh-Gal*4
- *hsFLP*1.22; *act-FRT < STOP > FRT-lacZ*/+; $UAS\text{-}Smad2^{SDVD}$/*hh-Gal*4
- 638-*Gal*4/+; *FRT42D* $babo^{32}$/*FRT42D* [*arm-lacZ*] $M(2)l^2$; *UAS-FLP*/+
- 638-*Gal*4/+; *FRT42D* $babo^{k16912}$/*FRT42D* [*arm-lacZ*] $M(2)l^2$; *UAS-FLP*/+.

Wing and cell size measurements

We analysed at least 10 wings from females of each genotype. Cell size was estimated from the number of trichomes in a dorsal region located in the interveins L3/L4 or L5/posterior margin (see Supplementary Fig. 1). Wing size was measured in pixels using the *Analyse* tool in Adobe Photoshop. The number of cells was calculated using cell density and wing size values. Wing pictures were made with a Spot digital camera coupled to

a Zeiss Axioplam microscope using the 5X and 20X objectives for wing sizes and trichome number, respectively.

Immunocytochemistry

We used mouse monoclonals anti-Wg, anti-Dlg, anti-Ptc and anti-Elav from the Hybridoma bank at Iowa University, rabbit anti-P-Mad and guinea pig anti-Brk (gifts from F. Martín and G. Morata), guinea pig anti-Dll (Estella et al., 2008), mouse anti-Bs anti β-Gal (Promega), rabbits anti-Sal (de Celis et al., 1996), anti β-Gal (Cappel), anti-activated Cas3 (Cell Signalling Technology), anti-Phosphorylated Histone 3 (PH3; Cell Signalling Technology), anti-Mira (a gift from C. Doe) and anti-P-Smad2 (Persson et al., 1998), kindly provided by Peter ten Dijke. In this last case we fixed the larvae in cooled 4% Formaldehyde, and keep them at least 24 h at −20 °C in Methanol. We also used Alexa Fluor 488® phalloidin and phalloidin-TRITC (Sigma) and TOPRO (Invitrogen). Secondary antibodies were from Jackson Immunological Laboratories (used at 1/200 dilution). Imaginal wing discs were dissected, fixed and stained as described in de Celis (1997). Confocal images were captured using a LSM510 confocal microscope. In most figures we show single confocal planes taken at the position of maximal signal intensity. The number of PH3 cells was quantified on projections of 10 confocal planes, and the orthogonal sections and analysis of fluoresce intensity (grey values) were made out using ImageJ 1.46n software (NIH, USA).

In situ hybridisation

In situ hybridisation with RNA probes was carried out as described in de Celis (1997). We introduced a Proteinase K treatment after the fixation (4 min using Proteinase K at 30 μg/ml) to improve probe penetration in the larval brains. The probes were synthesise from the following cDNAs: RE53485 (*Smad2*), GH14433 (*daw*), RE69013 (*mav*) and LD29161 (*myo*). We also used genomic DNA to generate probes using the following primers that contain T3 and T7 sequences (underlines sequences):

act*β*: 5′-TAATACGACTCACTATAGGGAGGGATCCAATGCTAGAGCGACCTT-3′ and 5′-ATTAACCCTCACTAAAGGGAGGGATCCAATGCTAGAGCGACCTT-3′

mav: 5′-TAATACGACTCACTATAGGGAGGGCCAGGATCTAGGAAAA-3′ and 5′-ATTAACCCTCACTAAAGGGAACATCTTCCGTGGCAGTACC-3′

Smad2: 5′-TAATACGACTCACTATAGGGGGCTATATGAGCGAGGATGG-3′ and 5′-ATTAACCCTCACTAAAGGGAGATGGAGTTCGATCCAGCAG-3′.

RNA isolation and quantitative real-time RT-PCR

In the case of *actβ* total RNA was isolated from 50 wild type wing imaginal discs as described in Molnar et al. (2011). To detect *actβ* mRNA, we made 8 qRT-PCR experiments using retrotranscribed cDNA as template (RT+) and 8 control qRT-PCR experiments using total RNA (RT−). In both cases we used the primers 5′-CCTGACAAGCTGCATACTCCT-3′ and 5′-CGTGCACTGTCCTACTGCTG-3′. We compared the results of the RT+ and RT− experiments using a Wilcoxon non-parametric test for paired samples. In the cases of *Smad2*, *babo*, *daw*, *mav* and *myo*, total RNA was isolated from a pool of 20 wild type and 20 mutant third instar larvae (*da-Gal4/UAS-Smad2-i*, *da-Gal4/UAS-babo-i*, *UAS-dicer2*; *da-Gal4/UAS-daw-i*, *UAS-dicer2*; *da-Gal4/UAS-mav-i* and *da-Gal4/UAS-myo-i*) following a TRIzol extraction protocol (Life Technologies; Grand Island, NY). After a DNAse treatment (DNA-free Dnase Tratment and Removal Reagents, Applied Biosystems), total RNA (1 μg) was used for a first round of reverse transcription employing the Superscript III First Strand Synthesis Supermix kit for qRT-PCR (Invitrogen). Quantitative PCR analysis was performed in a Cfx 384 Real-Time System (BioRad) using the following primers:

Smad2 5′-GTGGTGGTCCCTCCTCGT-3′ and 5′-TGCTGTTGCTGTTGATAGGC-3′; *babo* 5′-CAGACTTTGAACTTGCGACGC-3′ and 5′-GCAGCCCGAGAGCTTTTCTTT-3′; *babo-RA* (specific for the isoform RA) 5′-ATTATGTGCCACACCGACTG-3′ and 5′-CCGTGAAGCAAATGAAGAGG-3′; *daw* 5′-GGTGGATCAGCAGAAGGACT-3′ and 5′-GCCACTGATCCAGTGTTTGA-3′; *mav* 5′-TGAAGGGCCTTGGAATTAAA-3′ and 5′-TGTTGCCCTTCTCCTGGTTA-3′; *myo* 5′-GGCGACCACATAATGACTGA-3′ and 5′-TTAGCATCATCTCCCTGCATT-3′.

To normalise the results we used probes for the genes *Act42A*, *Tub84A* and *RPL32*. Three independent experiments were done and the quantification of cDNA reduction were compared using Student's *t*-test. A p-value ≤ 0.05 was considered to be statistically significant.

Fluorescence activated cell sorting (FACS)

We incubated wing imaginal discs of *en-Gal4 UAS-GFP/UAS-Smad2-i*; *en-Gal4 UAS-GFP/UAS-Smad2^{SDVD}* and *en-Gal4 UAS-GFP/+* (control discs) in 300 μl of trypsin solution (Tripsin-EDTA Sigma T4299) and 0.5 μl Hoescht (Hoescht33342, Trihydrochloride Trihydrate H3570, Molecular Probes™) at 28 °C during 40 min. We stopped the trypsin reaction with 200 μl of 1% FCS (Fetal Bovine Serum Sigma™ 9665). The cells were suspended in 300 μl of 1% FCS and the cell cycle profiles of GFP positive and GFP negative cells was quantified with a FACS Vantage 2 (Becton Dickinson™). The cell cycle profile of 7 independent experiments for each genotype was analysed using FloJow 7.5. We quantified for each genotype the GFP^+ (mutant)/GFP^- (control) ratio of the cells in each phase of the cycle (G1, S, G2).

Statistical analysis

All numerical data including wing size, imaginal disc size, cell size, cell number and intensity values were collected and processed in Microsoft Excel (Microsoft Inc.). The data were expressed as means +/− standard error of the mean (SEM) and were analysed using a *T*-test (Supplementary Table 1). We consider significant p-values lower than 0.01 (***), 0.025 (**) and 0.05 (*).

Results

Functional requirements of Smad2 and Babo during wing development

The expression in the wing disc of RNA interference against the three Drosophila Smads (*Smad2*, *Mad* and *Med*) recapitulates the known requirements of the TGFβ and BMP pathways during the growth and patterning of the wing. Thus, *Smad2* RNAi (*nub-Gal4/UAS-Smad2-i*) causes the formation of smaller than normal wings that differentiate a normal pattern of veins with minor vein thickening in distal regions of the L5 vein (Fig. 1A–B, E). *Mad* RNAi (*nub-Gal4/UAS-Mad-i*) also reduces the size of the wing and in addition prevents the differentiation of veins (Fig. 1C), and knockdown of *Med* (*nub-Gal4/UAS-Med-i*) results in a similar phenotype to loss of *Mad* (Fig. 1D). Complementary, the expression of phospho-mimic forms of Smad2 ($Smad2^{SDVD}$) and Mad (Mad^{SDVD}), which simulate a constitutively active form of the proteins (Gesualdi and Haerry, 2007), results in an increase in the size of the domain of ectopic expression and minor vein thickening (*en-Gal4/UAS-Smad2^{SDVD}*; Fig. 1F), and in the differentiation of ectopic veins (*en-Gal4/UAS-Mad^{SDVD}*; Fig. 1G). Interestingly, loss of *Smad2* or expression of $Smad2^{SDVD}$ also affect the size of the cells in opposite directions, causing the formation of larger than

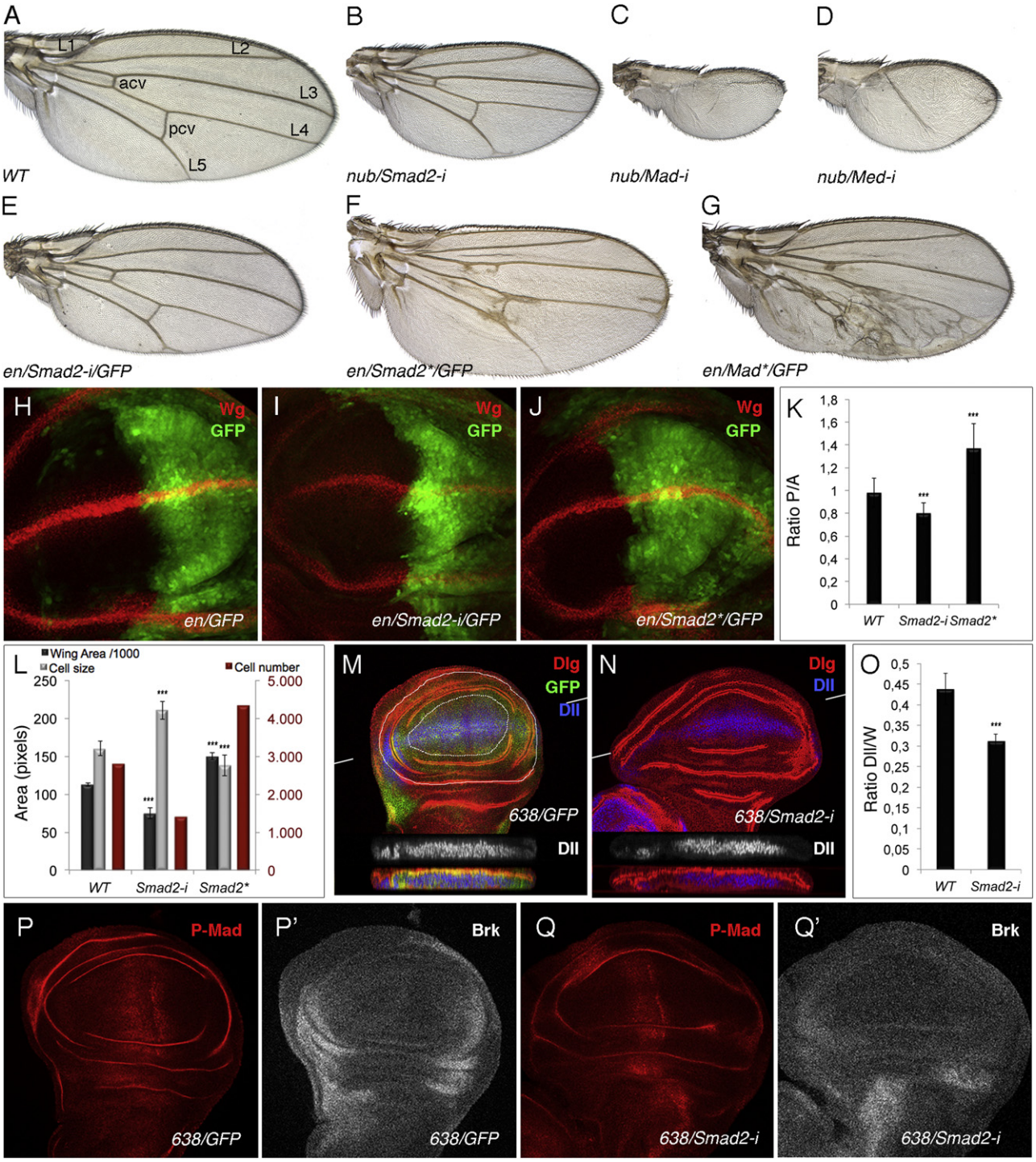

Fig. 1. Phenotype of loss and gain of function conditions in TGFβ and BMP pathway components. (A) Wild type wing showing the position of the longitudinal veins (L1–L5) and anterior (acv) and posterior crossveins (pcv). (B–D) Wings in which the expression of *Smad2* (*nub-Gal4/+;UAS-Smad2-i/+*, *nub/Smad2-i* in B), *Mad* (*nub-Gal4/+;UAS-Mad-i/+*, *nub/Mad-i* in C) and *Med* (*nub-Gal4/+;UAS-Med-i/+*, *nub/Med-i* in D) is reduced in the wing blade and hinge. (E–G) Autonomous, compartment-specific effects of posterior loss of *Smad2* (*en-Gal4 UAS-GFP/+;UAS-Smad2-i/+*, *en/Smad2-i/GFP* in E), posterior expression of $Smad2^{SDVD}$ (*en-Gal4 UAS-GFP/+;UAS-*$Smad2^{SDVD}$*/+, *en/Smad2*/GFP* in F) and posterior expression of Mad^{SDVD} (*en-Gal4 UAS-GFP/+;UAS-*Mad^{SDVD}*/+*, *en/Mad*/GFP* in G). (H–J) Posterior compartment-specific effects of changes in *Smad2* expression in posterior cells (green) in third instar wing discs of *en-Gal4 UAS-GFP/+* (*en/GFP*, H), *en-Gal4 UAS-GFP/+;UAS-Smad2-i/+* (*en/Smad2-i/GFP*, I) and *en-Gal4 UAS-GFP/+;UAS-*$Smad2^{SDVD}$*/+* (*en/Smad2*/GFP*, J). The expression of Wingless (Wg) is shown in red. (K) Ratio of posterior versus anterior compartment size in controls discs *en-Gal4 UAS-GFP/+* (WT; $n=10$), *en-Gal4 UAS-GFP/+; UAS-Smad2-i/+* (Smad2-i; $n=10$) and *en-Gal4 UAS-GFP/+; UAS-*$Smad2^{SDVD}$*/+* (Smad2*; $n=10$). (L) Wing size (black columns), Cell size (grey columns) and estimated number of cells (red columns) in control wings (*nub-Gal4/+*; WT), *nub-Gal4/+;UAS-Smad2-i/+* (*Smad2-i*) and *nub-Gal4/+; UAS-*$Smad2^{SDVD}$*/+* (Smad2*). (M–N) Expression of Distal-less (Dll, blue), Disc large (Dlg, red) and GFP (green in M) in control (*638-Gal4/+; UAS-GFP/+*, M) and *638-Gal4/+; UAS-Smad2-i/+ discs* (N). Below each image are shown the orthogonal sections taken at the plane indicated by white lines. (O) Average ratio between the area of Dll expression (Dll) in the wing pouch (dotted inner white line in M) and the wing (W; outer white line in M) in control (*638-Gal4/+*) and *638-Gal4/+; UAS-Smad2-i/+* wing discs ($n=7$). (P–Q′) Expression of P-Mad (red in P and Q) and Brk (white in P′ and Q′) in control discs (*638-Gal4/+; UAS-GFP/+*, P–P′) and Smad2-i (*638-Gal4/+; UAS-Smad2-i/+*, Q–Q′). The white arrows (Q′) indicate the places where Brk expression is reduced.

normal cells (*Smad*2-*i*) or smaller than normal cells ($Smad^{SDVD}$) (Fig. 1L; Supplementary Table 1). In this manner, loss of TGFβ activity affects cell growth and cell number, resulting in the formation of smaller than normal wings formed by a reduced number of larger than normal cells. Changes in Mad activity also modify cell size, but in this case both loss of Mad and expression of $Mad2^{SDVD}$ increased cell size in the L3/L4 region (Supplementary Table 1). The changes in wing size observed in adult wings after manipulations of *Smad*2, *Mad*, *Babo* and *Tkv* expression are already present in third instar wing discs (Fig. 1H–K and data not shown).

It was previously reported that a reduction in *Smad*2 expression causes overgrowth of the disc, a phenotype related to ectopic BMP signalling (Sander et al., 2010; Martin et al., 2004). We further analysed wing discs of 638-*Gal*4/*UAS-Smad*2-*i* genotype, and confirmed that these discs display abnormal morphologies (Fig. 1M–N). Using Distal-less (Dll) as a marker of the wing blade (Fig. 1M–N), we found a strong reduction in its domain of expression relative to the rest of the wing region of the disc (Fig. 1O and Supplementary Fig. 1). Therefore, loss of *Smad*2 in the 638-*Gal*4 domain of expression reduces the size of the wing pouch, and simultaneously causes an expansion of the lateral regions of the wing disc (Fig. 1M–O). The, reduced growth of the wing pouch is compatible with a requirement for Smad2 to mediate the growth-promoting effects of Babo (Brummel et al., 1999, see below). The phenotype of lateral expansion of the disc, however, is never observed in *babo* mutants (see below), but it is characteristic of ectopic Dpp signalling, being associated to the loss of *brinker* (*brk*) expression in these territories (Martin et al., 2004; Affolter and Basler, 2007; Schwank et al., 2008). In 638-*Gal*4/*UAS-Smad*2-*i* discs, we could not detect ectopic P-Mad expression in the lateral regions (Fig. 1P, Q), but we did see a consistent reduction in Brk expression levels (Fig. 1P′ and Q′).

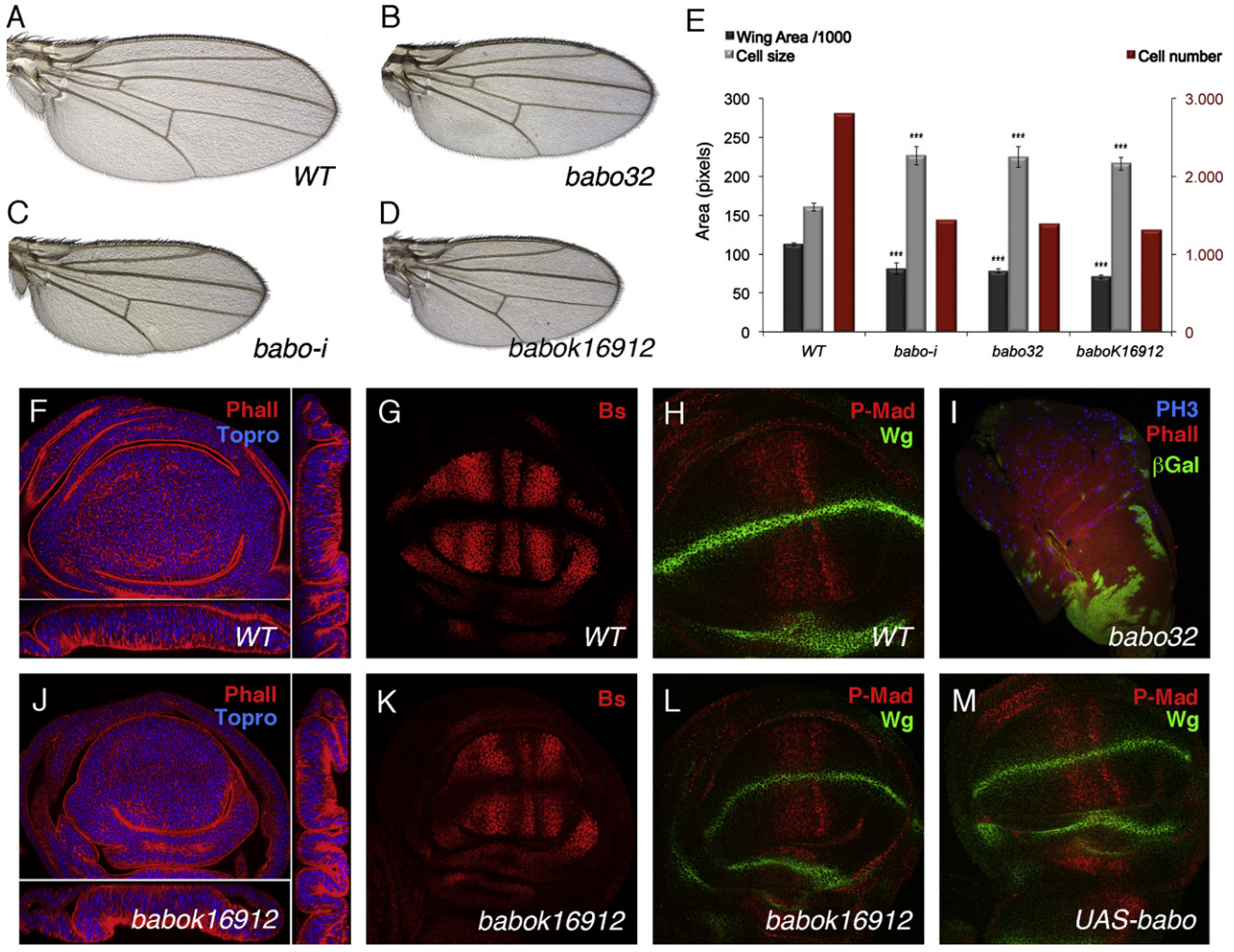

Fig. 2. Genetic analysis of *babo* mutants. (A) Wild type wing. (B) $babo^{32}$ homozygous mutant wing from 638-*Gal*4/+; *FRT*42*D* $babo^{32}$/*FRT*42*D* $M(2)l^2$ *P*[*arm-lacZ*]; *UAS-FLP*/+ females (*babo*32). (C) *nub-Gal*4/+; *UAS-babo-i*/+ wing (*babo-i*). (D) $babo^{k16912}$ homozygous mutant wing from 638-*Gal*4/+; *FRT*42*D* $babo^{k16912}$/*FRT*42*D* $M(2)l^2$ *P*[*arm-lacZ*]; *UAS-FLP*/+ females (*babok*16912). In B and D, the expression of FLP in the wing blade driven by 638-*Gal*4 generates homozygous *FRT*42 *babo* mutant cells that grow and occupy the entire wing blade (see also panel I). (E) Quantification of wing size (black columns, numerical values to the left $\times 10^3$), cell size (grey columns, numerical values to the left) and estimated number of cells (red columns, numerical values to the right) in wings of *nub-Gal*4/+;*UAS-GFP*/+ (*WT*), *nub-Gal*4/+;*UAS-babo-i*/+ (*babo-i*), 638-*Gal*4/+; *FRT*42*D* $babo^{32}$/*FRT*42*D* $M(2)l^2$; *UAS-FLP*/+ (*babo*32) and 638-*Gal*4/+; *FRT*42 $babo^{k16912}$/*FRT* $M(2)l^2$; *UAS-FLP*/+ (*baboK*16912) ($n=10$). (F–H) Wild type third instar wing disc showing the expression of Topro (blue) and Phalloidin (red) with the orthogonal sections to the right and to the bottom (F), the expression of the intervein marker Blister (Bs, red in G) and the expression of P-Mad and Wingless (red and green in H). (I) 638-*Gal*4/+; *FRT*42*D* $babo^{k16912}$/*FRT*42*D* $M(2)l^2$ *P*[*arm-lacZ*]; *UAS-FLP*/+ third instar disc showing the expression of βGal (green), Phalloidin (red) and PH3 (blue). Note that most of the wing disc, including the wing blade and hinge is formed by *babo* mutant cells. (J–L) Homozygous $babo^{k16912}$ third instar wing disc showing the expression of Topro (blue) and Phalloidin (red) with the orthogonal sections to the right and to the bottom (J), the expression of the intervein marker Blister (Bs, red in K) and the expression of P-Mad and Wingless (red and green in L). (M) Expression of P-Mad (red) and Wingless (green) in *nub-Gal*4/+; *UAS-babo*/+ third instar disc. Note that *babo* mutant discs are smaller in size, but the expression of Bs, P-Mad and Wg is normal in *babo* mutants (K–L) and in *babo* over-expression conditions (M).

Mutations in babo cause the same phenotypes as expression of babo RNAi

It was known that *babo* mutant larvae form discs and wings of smaller than normal size (Brummel et al., 1999). We wanted to confirm whether this phenotype corresponds to a disc-autonomous function of *babo*, and also validate the use of RNAi to analyse the requirements of the receptor during wing disc development. We studied the phenotypes of mosaic *babo* homozygous wings that develop from heterozygous larvae (638-*Gal4*/+ *FRT42D babo*/*FRT42D M(2)l*^{2}; *UAS-FLP*/+, see Material and Methods and Fig. 2I), and found that *babo*^{32} (Fig. 2B) and *babo*^{k16912} (Fig. 2D) homozygous wings display identical phenotype of smaller wings than *babo* RNAi wings (Fig. 2C). In all cases, the wings are formed by a reduced number of cells, and these cells are larger in size than wild type cells (Fig. 2E). In addition, homozygous *babo*^{k16912} discs show a small wing blade area (Fig. 2J, compare with F), and a normal pattern of *blister* (Fig. 2K, compare with G), *wingless* (Fig. 2L, compare with H) and P-Mad (Fig. 2L, compare with H) expression. The same results are obtained upon expression of *babo* RNAi in the wing blade (*nub-Gal4*/*UAS-babo-RNAi*; not shown). In contrast to the consequences of *babo* loss of expression, the over-expression of *babo* (*nub-Gal4*/*UAS-babo*) does not affect the size or pattern of the adult wing (not shown), and results in a normal pattern of P-Mad and *wingless* expression (Fig. 2M).

Function of TGFβ signalling in the regulation of wing size

The main developmental consequences of loss of *babo* or *Smad2* expression are the reduction in wing size and the increase in cellular size. We analysed the proliferation of *babo* mutant cells by clonal analysis of two *babo* alleles, *babo*^{32} and *babo*^{k16912}. We found that mutant clones for these alleles are smaller than their wild type twins (Fig. 3A and I), suggesting that *babo* mutant cells divide at a slower pace that wild type cells. This was also observed in the case of cells expressing *Smad2 RNAi*. In this case, and to prevent the possible effects of cell competition, we analysed the proliferation of neutral clones growing in *Smad2-i* and normal contexts, by generating cell lineage clones in *hsFLP*/+; *actFRT*<*stop*>*FRTlacZ*/+; *UAS-Smad2-i*/*hh-Gal4* wing discs. In this genetic background, anterior cell lineage clones consist of wild type cells growing in a wild type background, and posterior cell lineage clones are composed by cells with reduced levels of *Smad2* growing in the same genetic context. We observed that the size of anterior clones was always larger than the size of posterior clones induced at the same developmental time (Fig. 3B). Conversely, when cell lineage clones were induced in larvae of *hsFLP*/+; *actFRT*<*stop*>*FRTlacZ*/+; *UAS-Smad2*^{SDVD}/*hh-Gal4* genotype, the size of posterior clones was always larger than the size of anterior clones (Fig. 3C). We did not observe cell death in wing discs where the expression/activity of Smad2 was manipulated in the posterior compartment (data not shown). All together, these data suggests that cells with lower levels of Smad2 divide slower than wild type cells, and that the opposite occurs when wing cells express the activated form of Smad2.

A change in the proliferation rhythm is compatible with alterations in the regulation of cell cycle progression. We measured the fraction of cells in mitosis in the posterior and anterior compartments of wing discs in which the expression of Smad2 was manipulated only in posterior cells (Fig. 3E–H). We could not find a significant reduction in the fraction of mitotic cells when we reduced Smad2 levels (*en-Gal4 UAS-GFP*/*UAS-Smad2-i*; Fig. 3F, H). The expression of the activated form of the protein in posterior cells (*en-Gal4 UAS-GFP*/*UAS-Smad2*^{SDVD}; Fig. 3G) weakly but significantly increases the fraction of cells in mitosis (Fig. 3H). Finally, we observed that there is no significant change in the fraction of cells in different phases of the cell cycle (G1, S and G2), comparing wild type anterior and mutant posterior compartments, or comparing posterior compartments in mutant and control discs (Fig. 3E′–G′ and J). In this manner, it seems that TGFβ signalling does not affect any specific transition in the cell cycle, and more likely affects simultaneously the length of both G1 and G2. Finally, we observed a small fraction of dying cells in *babo* mutant discs (Fig. 3D). Suppression of cell death does not modify the *babo* mutant phenotype (data not shown), indicating that cell death does not contribute to the reduction in size of *babo* mutant wings.

Genetic interactions between Babo/Smad2 and Tkv/Mad

Next, we wanted to confirm the known relationships between Babo and Smad2 and between Tkv and Mad in genetic combinations, and also to explore the possibility of cross-interactions between these two pathways, as phosphorylation of Mad by Babo has been described in cell culture experiments (Gesualdi and Haerry, 2007). We first aimed to rescue the phenotype caused by constitutively activated forms of Babo and Tkv by reducing the expression of Smad2 or Mad. We reasoned that loss of the corresponding R-Smad should prevail to the activation of the receptor. Expression of activated Babo in the centre of the wing (*sal*^{EPv}*-Gal4*/*UAS-babo*^{QD}) causes a moderate increase in wing size and small disturbances to the patterning of the L2 vein (Fig. 4A). The knockdown of *Smad2* in this background totally suppresses the extra-growth, and the resulting wings have the same size as wing expressing only RNAi against *Smad2* (Fig. 4B–C). These wings also show some alterations in the pattern of veins, differentiating ectopic L2 stretches and extra-veins in the L4/L5 intervein (Fig. 4B). Knockdown of Mad also corrects the phenotype of activated Babo, and this, conversely, corrects the loss of veins caused by knockdown of Mad (Fig. 4D, compare with 4A and 4K). These results confirm that Babo requires Smad2 to promote wing growth, and suggest that, during vein differentiation, Babo^{QD} can compensate a reduction in Mad function, either by promoting the activation of the remnant of Mad, or because higher levels of activated Smad2 can promote vein formation in the Babo^{QD}/Mad-i background. In addition, it seems that Mad function is also required for Babo^{QD} to promote wing growth (Fig. 4D).

Over-activation of Tkv in the central domain of the wing, which correspond to its normal domain of activity, causes the loss of adjacent wing territories and small disturbances to the pattern of veins (Fig. 4I). This phenotype is not modified by a reduction of *Smad2* (Fig. 4L), but it is totally suppressed by a reduction of *Mad* (Fig. 4J–K). Thus, it seems that all effects of Tkv are mediated by Mad, without any contribution of Smad2.

To further explore the relationships between Smad2 and Mad with the receptors Babo and Tkv, we aimed to rescue the consequences of receptor reduction by the expression of phospho-mimic forms of Smad2 and Mad. Loss of *babo* expression to a large extent recapitulates the results obtained with *Smad2-i*, resulting in the formation of smaller than normal wings formed by a reduced number of larger cells (Figs. 4E and 1). We found that the expression of Smad2^{SDVD} totally suppress the growth defect caused by loss of *babo* (Fig. 4E–F, compare also with 4G). The expression of Mad^{SDVD} also corrects the loss of *babo* phenotype, rescuing the reduction in wing size and causing the same alterations in the venation pattern as expression of Mad^{SDVD} alone (Fig. 4H and O). The phenotype of *tkv* knockdown has a component of ectopic Tkv signalling, manifested in the formation of thicker than normal veins, and of *tkv* loss-of-function, consisting in a reduction in wing size (Fig. 4M and Supplementary Fig. 2). The ectopic veins and reduced wing size are still present in

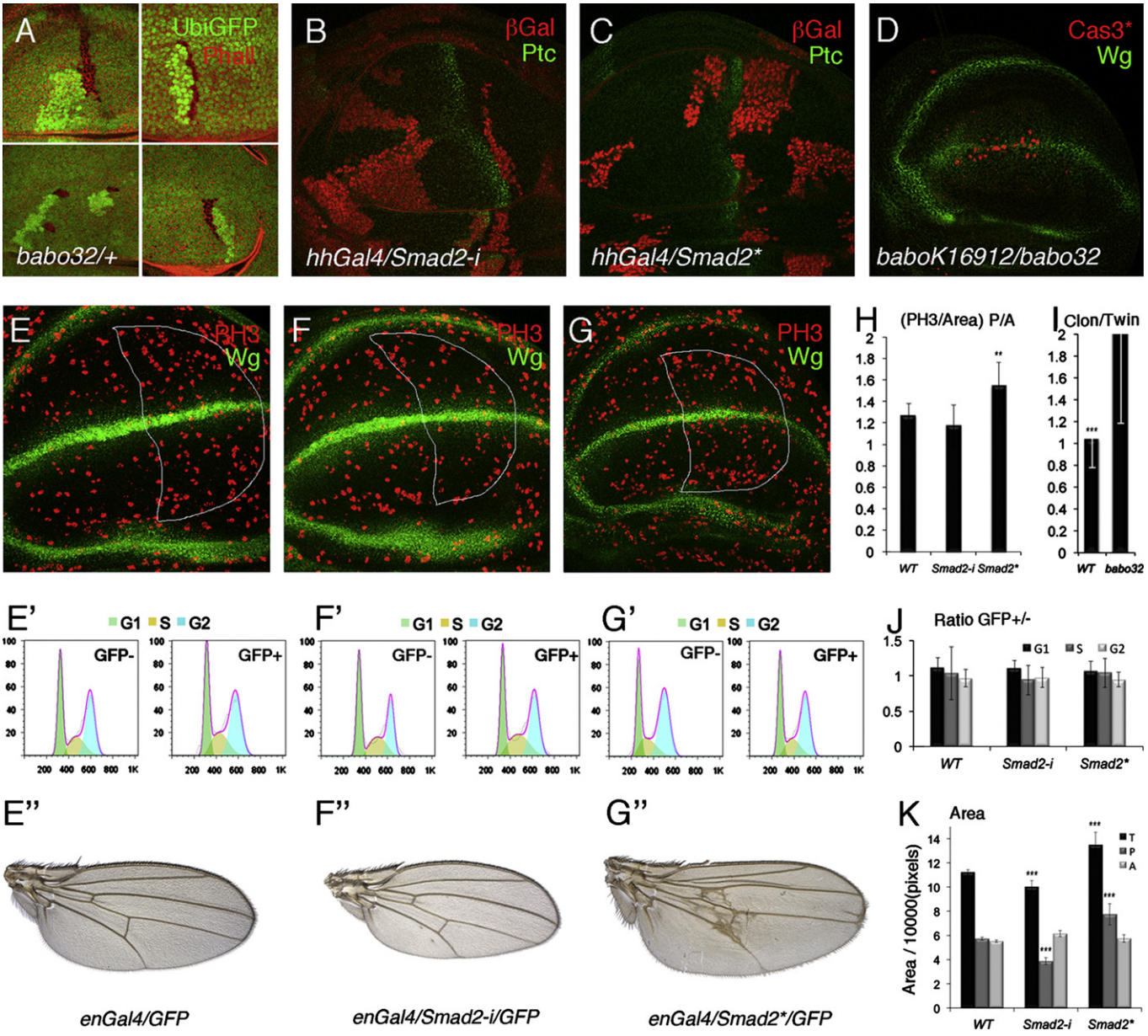

Fig. 3. Analysis of cell proliferation and cell death in *babo* and *Smad2* mutant wing discs. (A) Representative examples of *babo*^{32} clones (labelled by the absence of green) and their wild type twins (labelled in bright green) induced 48–72 h AEL in larvae of *hs-FLP*1.22/+; *FRT42D babo*^{32}/*FRT42D P*[*ubi-GFP*]/+ genotype. (B–C) Cell proliferation differences in the absence of cell competition, revealed by the size of cell lineage clones induced in *hs-FLP*1.22/+; *actFRT* < *stop* > *FRT lacZ*/+; *UAS-Smad2-i/hh-Gal*4 (B) and *hs-FLP*1.22/+; *actFRT* < *stop* > *FRT lacZ*/+; *UAS-Smad2*^{SDVD}/*hh-Gal*4 (C) larvae at 24–48 h AEL. Cell lineage clones are labelled in red (βGal) and the position of the anterior/posterior compartment boundary is labelled by the localisation of Patched (Ptc; green). (D) Cell death present in third instar wing discs of *babo*^{32}/*babo*^{k16912} genotype revealed by the expression of activated Cas3 (Cas3*, red). The expression of Wingless (Wg) is shown in green. We could not detect Cas3* expression in wild type discs of the same age (n=10). (E–G″) Analysis of mitosis and cell cycle in *en-Gal*4 *UAS-GFP*/+ (enGal4/GFP; E–E″), *en-Gal*4 *UAS-GFP*/+; *UAS-Smad2-i*/+ (*enGal4/Smad2-i/GFP*; F–F″) and *en-Gal*4 *UAS-GFP*/+; *UAS-Smad2*^{SDVD}/+ (*enGal4/Smad2*/GFP*; G–G″). (E–G) Third instar wing imaginal discs showing the expression of Wingless (Wg, green) and Phospho Histone 3 (PH3, red). The area of the posterior compartment is included in the area enclosed by the white line. (E′–G′) FACS analysis showing the GFP^{-} (control anterior, left panels) and GFP^{+} (posterior cells, right panels). (E″–G″) Adult wings. (H) Average ratio of PH3-expressing cells relative to the area of the posterior and anterior compartments (n=10). Same genotypes as in E–G. (I) Average clon/twin ratio in twin clones induced in larvae of *hs-FLP*1.22/+; *FRT42D/FRT42D P*[*ubi-GFP*]/+ (WT; n=37) and *hs-FLP*1.22/+; *FRT42D babo*^{32}/ *FRT42D P*[*ubi-GFP*]/+ (*babo*32; n=43). (J) Ratio between GFP^{+} and GFP^{-} cells in G1 (black columns), S (dark grey columns) and G2 (light grey) of 7 independent FACS experiments of the genotypes shown in E-G. (K) Average size of the wing blade (black columns), the posterior compartment (dark grey columns) and the anterior compartment (light grey columns) in wings of *en-Gal*4 *UAS-GFP*/+ (*WT*; n=10), *en-Gal*4 *UAS-GFP*/+; *UAS-Smad2-i*/+ (*Smad2-i*; n=10) and *en-Gal*4 *UAS-GFP*/+; *UAS-Smad2*^{SDVD}/+ (*Smad2**, n=10).

combination with Smad2^{SDVD} (Fig. 4P). The combination *tkv-i*+*Mad*^{SDVD} results in a phenotype indistinguishable to the expression of *Mad*^{SDVD} alone (Fig. 4N–O). Finally, we combined loss of both Smad2 and Mad, and observed the same loss of veins caused by loss of Mad, and a synergistic phenotype of wing size reduction (Supplementary Fig. 2). Although the results of combinations between hypomorphic conditions are not always clear-cut due to the nature of the manipulation, our results confirm the key contribution of Smad2 and Mad to Babo and Tkv signalling, respectively, and suggests coordinated but independent contributions of Smad2 and Mad to wing growth. Furthermore, the rescue of the *babo-i* by Smad2^{SDVD} suggests

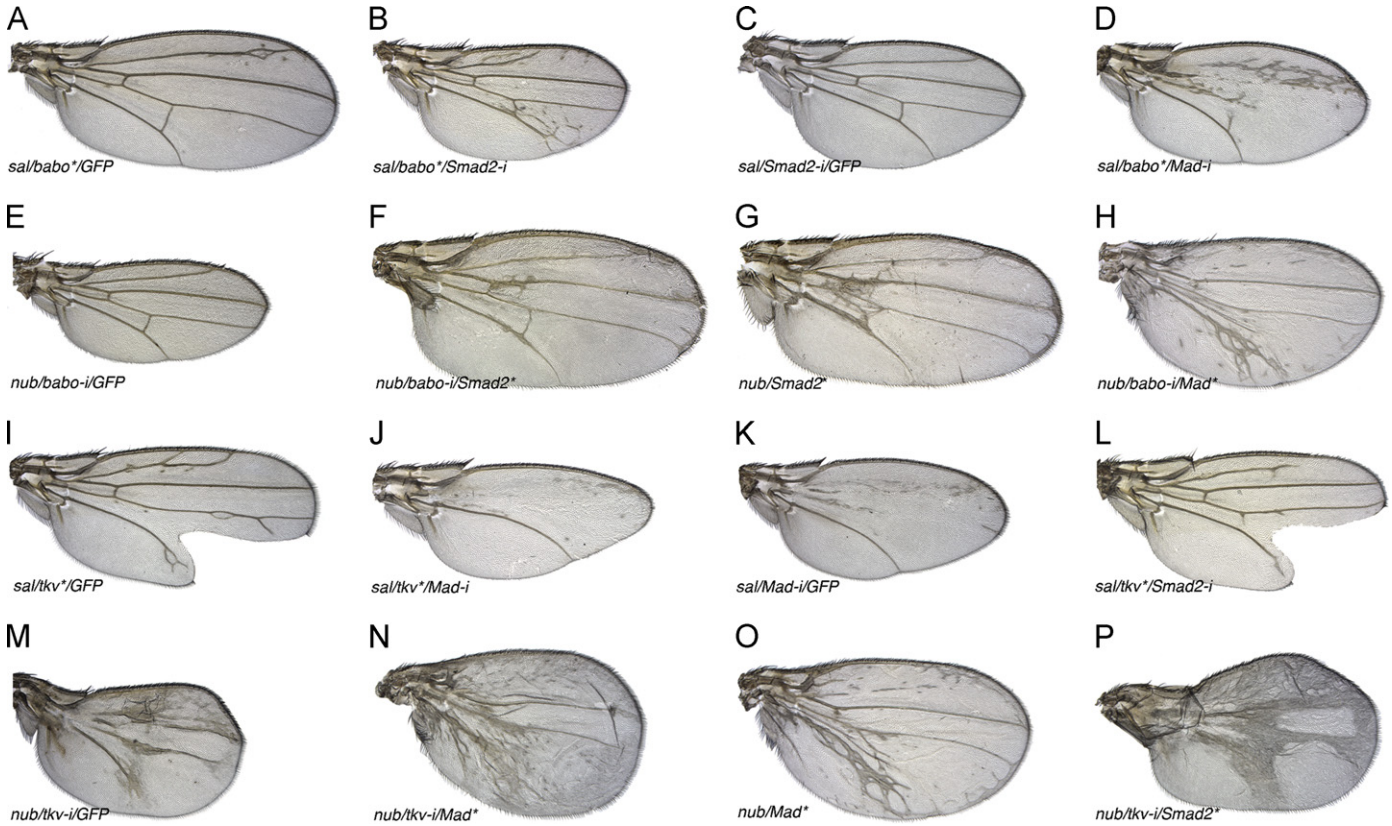

Fig. 4. Genetic epistasis between Smad2 and Mad with the type I receptors Tkv and Babo. (A–D) Modifications of the phenotype caused by the expression of activated Babo in the central region of the wing (*sal^{EPv}-Gal4/+*; *UAS-babo^{QD}/UAS-GFP*, *sal/babo*/GFP* in A), when combined with the loss of Smad2 (*sal^{EPv}-Gal4/+*; *UAS-babo^{QD}/UAS-Smad2-i*, *sal/babo*/Smad2-i* in B), or with the loss of Mad (*sal^{EPv}-Gal4/+*; *UAS-babo^{QD}/UAS-Mad-i*, *sal/babo*/Mad-i* in D). The loss of Smad2 (*sal/Smad2-i/GFP*) is shown in C (*sal^{EPv}-Gal4/+*; *UAS-GFP/UAS-Smad2-i*). (E–H) Rescue of the phenotype caused by loss of *babo* in the wing disc (*nub-Gal4/+*; *UAS-babo-i/UAS-GFP*, *nub/babo-i/GFP* in E) by the expression of phosphomimic Smad2 (*nub-Gal4/+*; *UAS-babo-i/UAS-Smad2^{SDVD}*, *nub/babo-i/Smad2** in F) and phosphomimic Mad (*nub-Gal4/+*; *UAS-babo-i/UAS-Mad^{SDVD}*, *nub/babo-i/Mad** in H). The combination *nub-Gal4/+*; *UAS-Smad2^{SDVD}/+* (*nub/Smad2**) is shown in G. (I–L) Modifications of the phenotype caused by the expression of activated Tkv (Tkv^{QD}) in the central region of the wing (*sal^{EPv}-Gal4/+*; *UAS-tkv^{QD}/UAS-GFP*, *sal/tkv*/GFP*, I), combined with the loss of Mad (*sal^{EPv}-Gal4/+*; *UAS-tkv^{QD}/UAS-Mad-i*, *sal/tkv*/Mad-i* in J) and Smad2 (*sal^{EPv}-Gal4/+*; *UAS-tkv^{QD}/UAS-Smad2-i*, *sal/tkv*/Smad2-i* in L). The loss of Mad (*sal/Mad-i/GFP*) is shown in K (*sal^{EPv}-Gal4/+*; *UAS-GFP/UAS-Mad-i*). (M–P) Modifications of the phenotype caused by reduction of *tkv* in the wing (*nub-Gal4/+*; *UAS-tkv-i/UAS-GFP*, *nub/tkv-i/GFP* in M) by the expression of phosphomimic Mad (*nub-Gal4/+*; *UAS-tkv-i/UAS-Mad^{SDVD}*, *nub/tkv-i/Mad** in N) and phosphomimic Smad2 (*nub-Gal4/+*; *UAS-tkv-i/UAS-Smad2^{SDVD}*, *nub/tkv-i/Smad2** in P). The combination *nub-Gal4/UAS-Mad^{SDVD}* is shown in O (*nub/Mad**). Activated versions of Mad, Smad2, Babo and Tkv are abbreviated with an asterisk.

that the phosphomimic form of Smad2 functions as a constitutively active protein.

Spatial domains of TGFβ activation

The domain of Tkv/Mad activity is restricted to a central region in the developing wing blade, where the phosphorylated form of Mad (P-Mad) is accumulated (Teleman and Cohen, 2000). To our knowledge, the domain of activity of Babo/Smad2 is still not known, although the global requirement of Smad2 suggests that it might be generalised in the wing disc. We used an antibody raised against the phosphorylated form of human Smad2 (Persson et al., 1998) that seems to recognise Drosophila Smad2. Thus, the signal obtained with this antibody is very much reduced in posterior cells when *Smad2* expression is reduced in the posterior compartment in *en-Gal4 UAS-GFP/+*; *UAS-Smad2-i/+* discs (Fig. 5A–A′). Conversely, expression of activated Babo in the same compartment, (*en-Gal4 UAS-GFP/+*; *UAS-babo^{QD}/+*) causes an increase in the level of P-Smad2 accumulation (Fig. 5C–C′). Using this antibody, we observed that P-Smad2 is detected in all wing disc cells, and that its accumulation is minimal along the presumptive wing margin and in the developing veins in late third instar discs (Fig. 5E). Cells expressing lower levels of P-Smad2 at this stage correspond to the zone of non-proliferation (O'Brochta and Bryant, 1985), suggesting a correspondence between cell division and expression of P-Smad2. P-Smad2 is also expressed at high levels in the nuclei of cells located posteriorly to the morphogenetic furrow in the eye disc, which might correspond to the developing photoreceptors (Fig. 5G) and in the ring gland (Fig. 5F). The expression of P-Smad2 is also robust in the developing brain (Supplementary Fig. 3), where the activity of the pathway is required to promote neuroblast proliferation and neuronal differentiation (Zheng et al., 2006; Zhu et al., 2008). The expression of a *Smad2* reporter, which shows a good correspondence with the accumulation of P-Smad2 in the brain (Supplementary Fig. 3), is mostly restricted to neurons, but it is also detected in some neuroblasts (Supplementary Fig. 3).

Expression and functional requirements of the candidate TGFβ ligands in the wing disc

There are four TGFβ-type ligands in the Drosophila genome, Actβ, Daw, Myo and Mav (Gesualdi and Haerry, 2007; Raftery and Sutherland, 1999). Previous studies showed that Actβ and Daw are able to induce phosphorylation of dSmad2 in S2 cells (Gesualdi and Haerry, 2007), and they appear to mediate the effects of *babo* during neuroblast proliferation and neuronal remodelling (Zhu et al., 2008). Furthermore Actβ is the only candidate ligand that reproduces, when over-expressed in the wing disc, the effects of activated Babo (Gesualdi and Haerry,

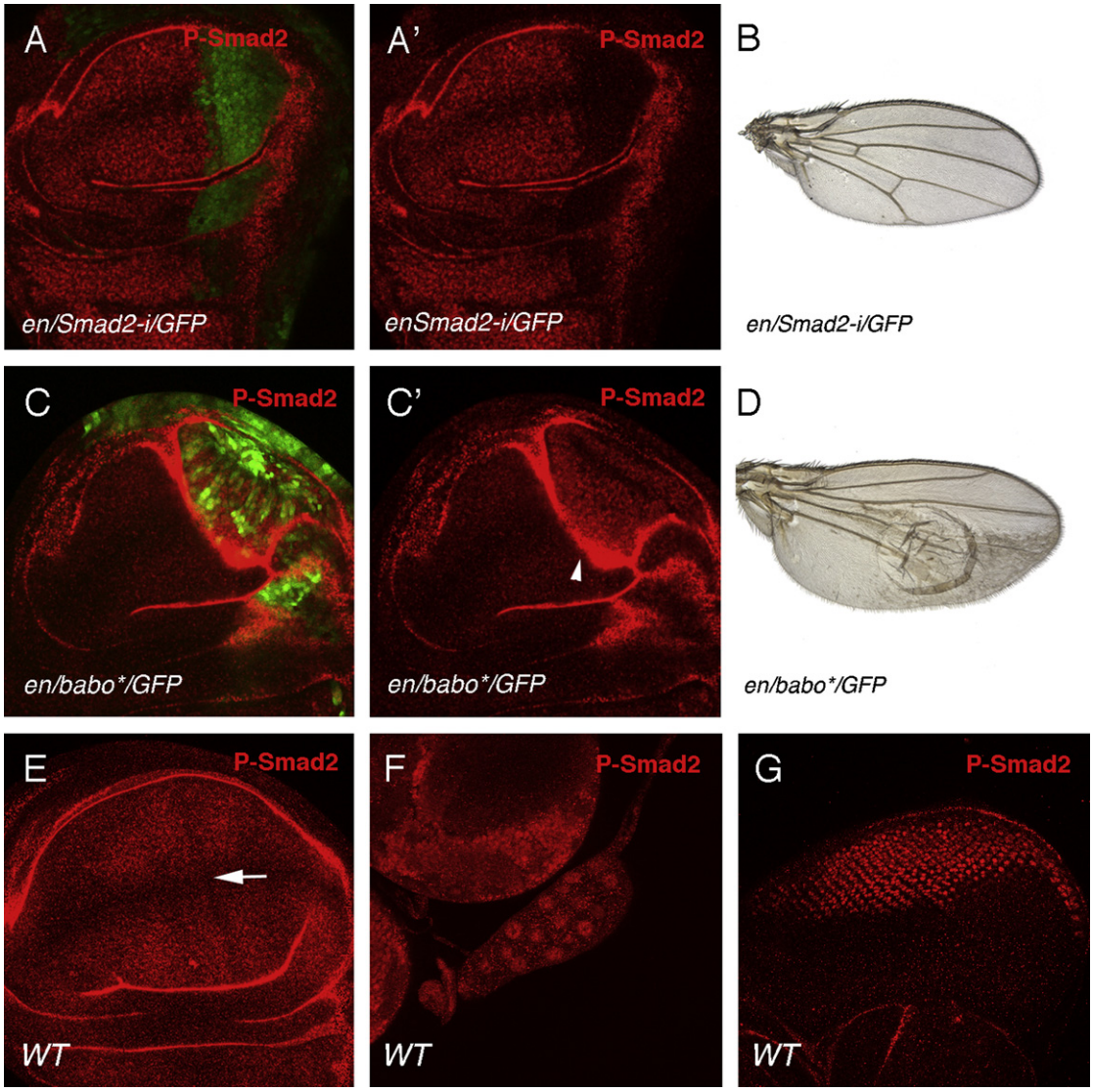

Fig. 5. Spatial domain of TGFβ activation in the wing disc. (A–A′) Loss of P-Smad2 expression (red) in posterior cells (labelled in green in A) of *en-Gal4 UAS-GFP/+;UAS-Smad2-i/+* wing discs (*en/Smad2-i/GFP*). The red channel showing only P-Smad2 is shown in A′. (B) Adult wing of *en-Gal4 UAS-GFP/+; UAS-Smad2-i/+* genotype showing a reduction in the size of the posterior compartment. (C–C′) Increase in P-Smad2 expression in posterior cells (labelled in green in C) of *en-Gal4 UAS-GFP/+; UAS-babo^{QD}/+* genotype (*en/babo*/GFP*) grown at 25 °C. The red channel showing only P-Smad2 is shown in C′. The intense red staining observed in anterior cells (white arrowhead in C') is located in the epithelial fold formed at the anterior-posterior compartment boundary and correspond to background. (D) Adult wing of *en-Gal4 UAS-GFP/+; UAS-babo^{QD}/+* genotype grown at 17 °C showing the differentiation of extra-vein tissue in a larger posterior compartment. (E–G) Expression of P-Smad2 in the wing disc (E), ring gland (F) and eye disc (G). The expression of P-Smad2 (red) is detected in all wing cells, but at much lower levels in the non-proliferating region of the presumptive wing margin (white arrow in A). In the eye disc, the expression of P-Smad2 is maximal in cells located posterior to the morphogenetic furrow that might correspond to photoreceptor cells (G), and in the ring gland is observed in the nuclei of all cells of the corpum allatum (F).

2007). It has been reported that *actβ* is not expressed in the wing disc (Gesualdi and Haerry, 2007), and conflicting results exits in the case of *daw* expression in this tissue (Gesualdi and Haerry, 2007; Parker et al., 2006). We analysed the expression of the four ligands by in situ hybridisation, and found that all of them are expressed in a generalised manner in the wing disc (Fig. 6B–E), and in more restricted patterns in the eye disc and larval brain (Supplementary Fig. 4). The expression of *Smad2*, *actβ*, *mav* and *myo* is also present during pupal development (Fig. 6A′–E′). We reduced the levels of ligand expression using RNA interference to identify their functional requirements (Supplementary Figs. 5 and 6). The expression of RNAi directed against each ligand in the wing blade and hinge (*nub-Gal4*) results in wings smaller in size than wild type, with stronger phenotypes observed upon reduction of *mav* or *myo* expression (Fig. 6B″–E″; see also Supplementary Figs. 5 and 6). In no case we could find the same reduction in wing size caused by reduced *Smad2* or *babo* expression, suggesting that the ligands display some redundancy in their abilities to activate Babo or that the reduction in expression levels observed upon RNAi expression (see Supplementary Fig. 6) is not enough to reveal their absolute requirements. Because of the hypomorphic nature of the RNAi approach, the synergistic reduction in wing size observed when we decreased simultaneously the expression of *daw* and *myo* (Fig. 6A″) is compatible with both interpretations. The double combinations *mav-i/myo-i* and *actβ-i/myo-i* resulted in additive phenotypes (see Supplementary Table 1). We also studied some of these combinations using a Gal4 driver expressed only in the wing blade (*Gal4-638*). Expression of *actβ-i*, *daw-i* or *myo-i* in the wing blade using this driver did not affected wing size (not shown), whereas expression of *mav-i* slightly reduced

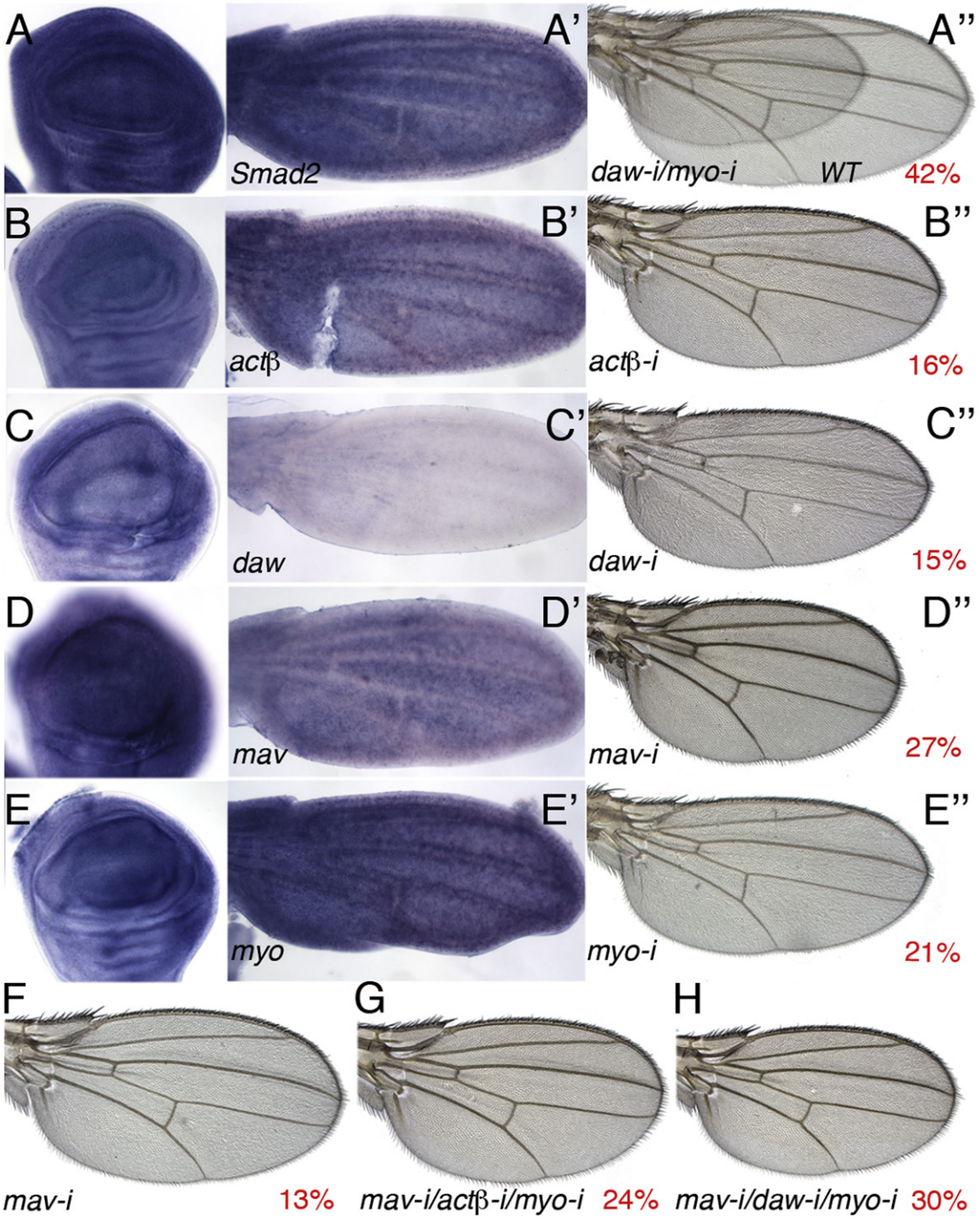

Fig. 6. Expression and requirements of TGFβ ligands in the wing disc. (A–A′) Expression of *Smad*2 mRNA in a third instar wing disc (A) and pupal wing 24–28 h APF (A″). (A″) Wild type wing and over-imposed mutant *nub-Gal4/UAS-daw-i*; *UAS-myo-i*/+ (*daw-i/myo-i*). (B–B′) Expression of *actβ* in wild type discs (B) and pupal wings 24–28 h APF (B′). (B″) Phenotype of *UAS-dicer*/+; *nub-Gal4/UAS-actβ* wings. (C–C′) Expression of *daw* in wild type discs (C) and pupal wings 24–28 h APF (C′). (C″) Phenotype of *UAS-dicer*/+; *nub-Gal4/UAS-daw-i* wings. (D–D″) Expression of *mav* in wild type discs (D) and pupal wings 24–28 h APF (D′). (D″) Phenotype of *UAS-dicer*/+; *nub-Gal4/UAS-mav-i* wings. (E–E″) Expression of *myo* in wild type discs (E) and pupal wings 24–28 h APF (E′). (E″) Phenotype of *UAS-dicer*/+; *nub-Gal4/UAS-myo-i* wings. (F–H) Wing size reductions observed in 638-*Gal*4 wings. 638-*Gal4*/+;*UAS-mav-i*/+ (*mav-i*; F). The triple combinations *638-Gal4*/+; *UAS-mav-i*/+; *UAS-actβ-i*/*UAS-myo-i* (*mav-i*/*actβ-i*/*myo-i*; G) and 638-*Gal4*/+; *UAS-mav-i*/+; *UAS-daw-i*/*UAS-myo-i* (*mav-i*/*daw-i*/*myo-i*; H) display a synergistic effect of wing size reduction. Unless otherwise stated, all combinations were grown at 29 °C. The percentage of wing size reduction relative to each control is indicated in red numbers in each panel ($n=10$).

wing size (Fig. 6F). The addition of *actβ-i*, *daw-i* or *myo-i* to the 638-*Gal4/UAS-mav-i* background increases the phenotype of *mav* knockdown (Fig. 6G–H; Supplementary Table 1). The pattern of veins observed in all combinations expressing RNA interference for the four ligands is always normal, suggesting that Tkv/Mad signalling is not affected by ligands of the TGFβ class.

Cross-interactions between TGFβ and BMP signalling in the wing

The over-expression of activated forms of Babo causes phenotypes not easily assignable to Smad2 activation. Thus, although Babo^{QD} increases the level of P-Smad2 (see Fig. 5C), this results in phenotypes not observed when phosphomimic forms of Smad2

are expressed in the same spatial domains (Fig. 1F). This was most clearly observed when Babo^{QD} is expressed in the posterior compartment of the disc, causing an unexpected reduction in the size of this compartment (Fig. 7C) and the formation of epithelial folds separating anterior and posterior cells (Supplementary Fig. 7). These phenotypes are reminiscent of confrontations between cells expressing different levels of BMP/Tkv signalling (Gibson and Perrimon, 2005). To clarify the effects of Babo^{QD}, we expressed this constitutively active form of the protein in different patterns and at different levels. Using three different Gal4 lines, *en-Gal4*, *nub-Gal4* and *sal^{EPv}-Gal4*, we found that in combinations grown at 17 °C (i.e. low level of over-expression), Babo^{QD} causes the expected growth phenotype associated to Smad2^{SDVD}, consisting in the formation of larger than normal wings (Fig. 7B, D, G). In addition, these wings show ectopic vein tissue, a phenotype not observed when Smad2^{SDVD} is expressed in the same pattern (see Figs. 1F and 4G). When we increased the levels of Babo^{QD} expression, by growing the flies at higher temperatures (25 °C and 29 °C), the size effects of Babo^{QD} are reversed, and the wings are progressively smaller. The pattern of veins in these wings is a mixture of loss of longitudinal veins and differentiation of extra-vein tissue (Fig. 7C, E–F, H–I).

Some of the phenotypes observed when Babo^{QD} is expressed at high levels could be caused by changes in P-Mad expression, and consequently we monitored the levels of P-Mad and the expression of some of its targets in these mutant backgrounds. In wild type discs, P-Mad is detected in a central stripe in the wing blade (Fig. 8A–A″), the same region that expresses the gen *spalt* (*sal*) (Fig. 8A–A′). In these cells, P-Mad is required to repress the expression of *brinker* (*brk*) (Campbell and Tomlinson, 1999; Jazwinska et al., 1999; Minami et al., 1999), which is expressed only in the peripheral regions of the wing disc (Fig. 8A, A‴, B). We found that at intermediate levels of Babo^{QD} expression (25 °C) there is already a considerable decrease in P-Mad accumulation (Fig. 8C–C″, F′ and M) and a concomitant expansion of *brk* expression (Fig. 8C, C‴, Supplementary Fig. 9). The expansion of *brk* is maximal when the levels of Babo^{QD} expression are higher (Fig. 8D, compare with 8B). At lower levels of Babo^{QD} expression, the domain of P-Mad is present, but the levels of P-Mad are reduced (Fig. 8F, compare with 8E and 8M). These data indicate that Babo^{QD} reduces the phosphorylation of Mad. Surprisingly; the effects of Babo^{QD} on P-Mad accumulation are completely reversed when *Smad2* expression is reduced. Thus, in *nub-Gal4/UAS-babo^{QD} UAS-Smad2-i* discs, P-Mad is now detected at high levels in the entire wing blade (Fig. 8G, G′ and M). Actually, this pattern of P-Mad accumulation is similar to that observed when a constitutively active form of Tkv (Tkv^{QD}) is expressed in the wing blade (*nub-Gal4/UAS-tkv^{QD}*; Fig. 8H, H′ and M). As expected from these effects on P-Mad, adult wings expressing Babo^{QD} in a background of reduced *Smad2* (Fig. 8J) are undistinguishable from wings expressing ubiquitously Tkv^{QD} or the Tkv ligand Dpp (Fig. 8L and K, respectively). In this manner, it seems that Babo^{QD} has the potential to phosphorylate Mad, but that this effect only occurs when Smad2 is not available. As mentioned before, we did not find any effect on Mad phosphorylation by over-expression of a normal version of Babo (Fig. 2M) or by reducing *Smad2* expression (Fig. 1Q–Q′).

Punt level of expression influences the antagonism of Babo^{QD} on Mad phosphorylation

BMP and TGFβ signalling share some of its components, mainly the type II co-receptor Put and the Smad4 protein Medea. We checked whether the interference caused by Babo^{QD} on Mad phosphorylation and Dpp signalling depends on the expression levels of Put. The expression of higher than normal levels of Put results in small wings in which all cells differentiate as veins (Fig. 9B′, compare with Fig. 9A′), and the expression of P-Mad is detected in the entire wing pouch (Fig. 9B, compare with 9A). As mentioned before, the expression of Babo^{QD} also reduces wing

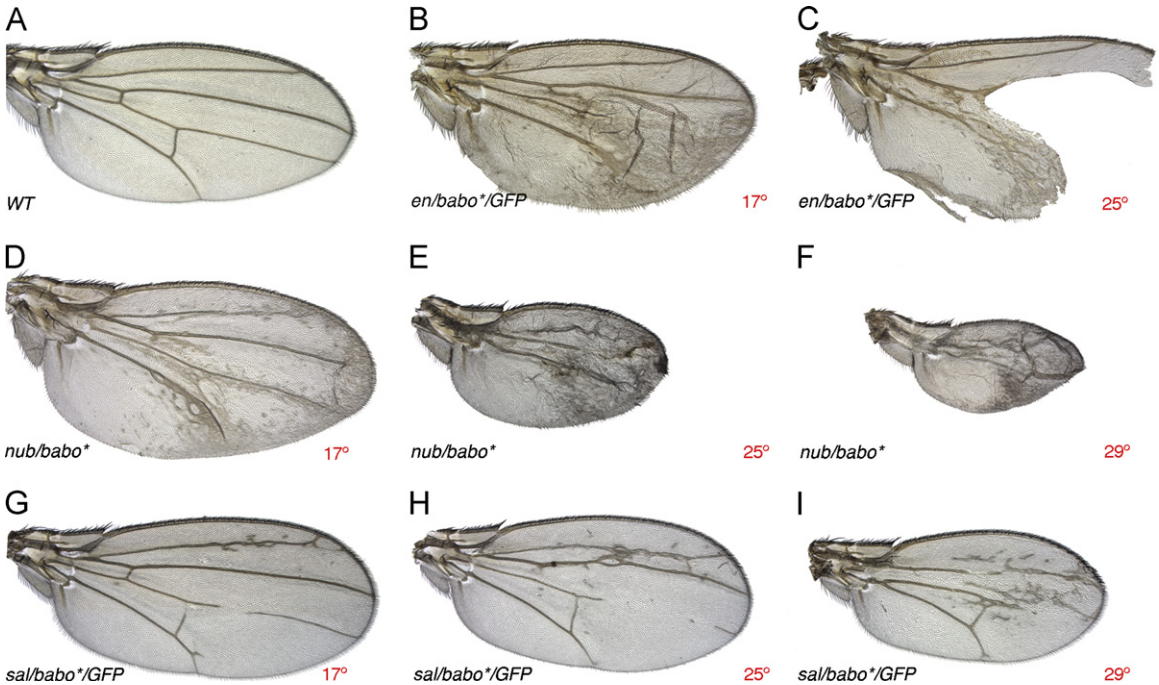

Fig. 7. Expression of a constitutively activated form of Babo causes loss of Dpp/BMP function phenotypes. (A) Wild type wing (WT). (B–C) *en-Gal4 UAS-GFP/+;UAS-babo^{QD}/+* wings (*en/babo*/GFP*) in flies grown at 17 °C (B) and 25 °C (C). (D–F) *nub-Gal4/+; UAS-babo^{QD}/+* wings (*nub/babo**) in flies grown at 17 °C (D), 25 °C (E) and 29 °C (F). (G–I) *sal^{EPv}-Gal4/+; UAS-GFP/UAS-babo^{QD}* wings (*sal/babo*/GFP*) in flies grown at 17 °C (G), 25 °C (H) and 29 °C (I). At higher levels of Babo^{QD} expression, the size of the wing is smaller, and the longitudinal veins fail to differentiate.

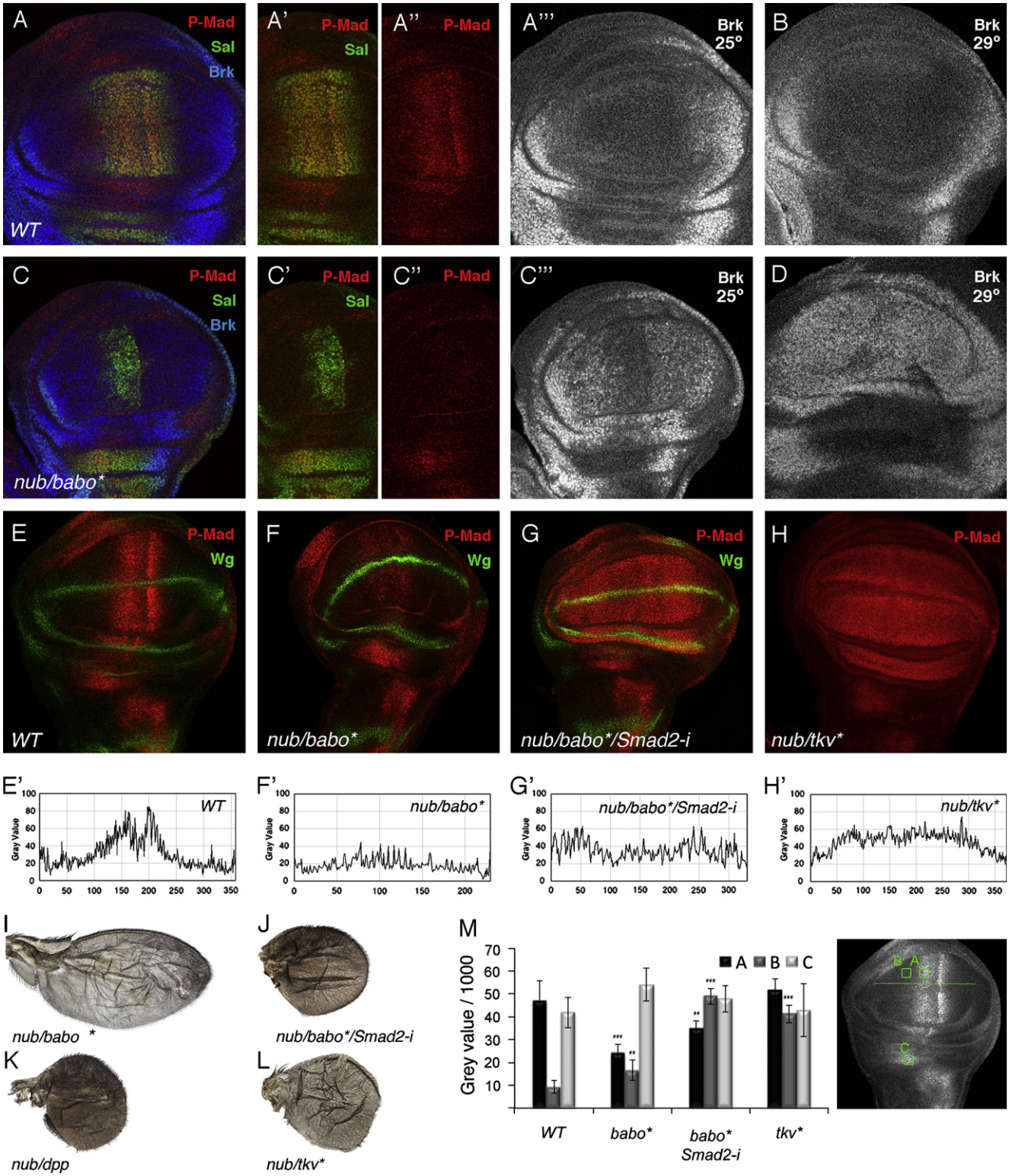

Fig. 8. Changes in Babo and Smad2 expression modify Dpp/BMP signalling. (A–A‴) Third instar wild type disc grown at 25 °C showing the expression of Brk (blue), Sal (green) and P-Mad (red). The expression of Sal and P-Mad is also shown in A′, and the expression of P-Mad and Brk in A″ and A‴, respectively. (B) Expression of Brk in a wild type disc grown at 29 °C. (C–C‴) Expression of Brk (blue), Sal (green) and P-Mad (red) in a third instar disc of *nub-Gal4/+*; *UAS-babo^{QD}/+* genotype grown at 25 °C. The expression of Sal and P-Mad is also shown in C′, and the expression of P-Mad and Brk in C″ and C‴, respectively. (D) Expression of Brk in *nub-Gal4/+*; *UAS-babo^{QD}/+* third instar wild type disc grown at 29 °C (compare with B). (E–H) Expression of P-Mad (red) and Wingless (green) in wild type third instar discs (WT; E), *nub-Gal4/+*; *UAS-babo^{QD}/+* discs (*nub/babo**; F), *nub-Gal4/+*;*UAS-babo^{QD}/UAS-Smad2-i* discs (*nub/babo*/Smad2-i*; G) and *nub-Gal4/UAS-tkv^{QD}* discs (*nub/tkv**; H). (E′–H′) Fluorescence intensity profiles of P-Mad expression along the anterior-posterior axes of the wing pouch (green line in the disc shown in M) of the wing discs shown in E–H. Note that the level of P-Mad expression is strongly reduced by Babo^{QD} expression (F–F′), and expanded throughout the wing pouch in the combination *Babo^{QD}/Smad2-i* (G–G′) and Tkv^{QD} (H–H′). Discs were taken with the 40x objective and the zoom set at 0.7 (A–D), or with the 25x objective (E–H). (I) Adult wing of *nub-Gal4/+*;*UAS-babo^{QD}/+* genotype grown at 25 °C (*nub/babo**). (J) Adult wing of *nub-Gal4/+*; *UAS-babo^{QD}/UAS-Smad2-i* genotype grown at 25 °C (*nub/babo*/Smad2-i*). (K–L) Adult wings of *nub-Gal4/+*;*UAS-dpp/+* (*nub/dpp*; K) and *nub-Gal4/+*;*UAS-tkv^{QD}/+* (*nub/tkv**; L) genotypes grown at 25 °C. These wings are very similar to each other, and also similar to the wing shown in J. (M) Quantification of P-Mad expression in three regions of the wing pouch (green squares in the disc shown to the right) of 5 discs of the genotypes shown in E (WT), F (*babo**), G (*babo*/Smad2-i*) and H (*tkv**).

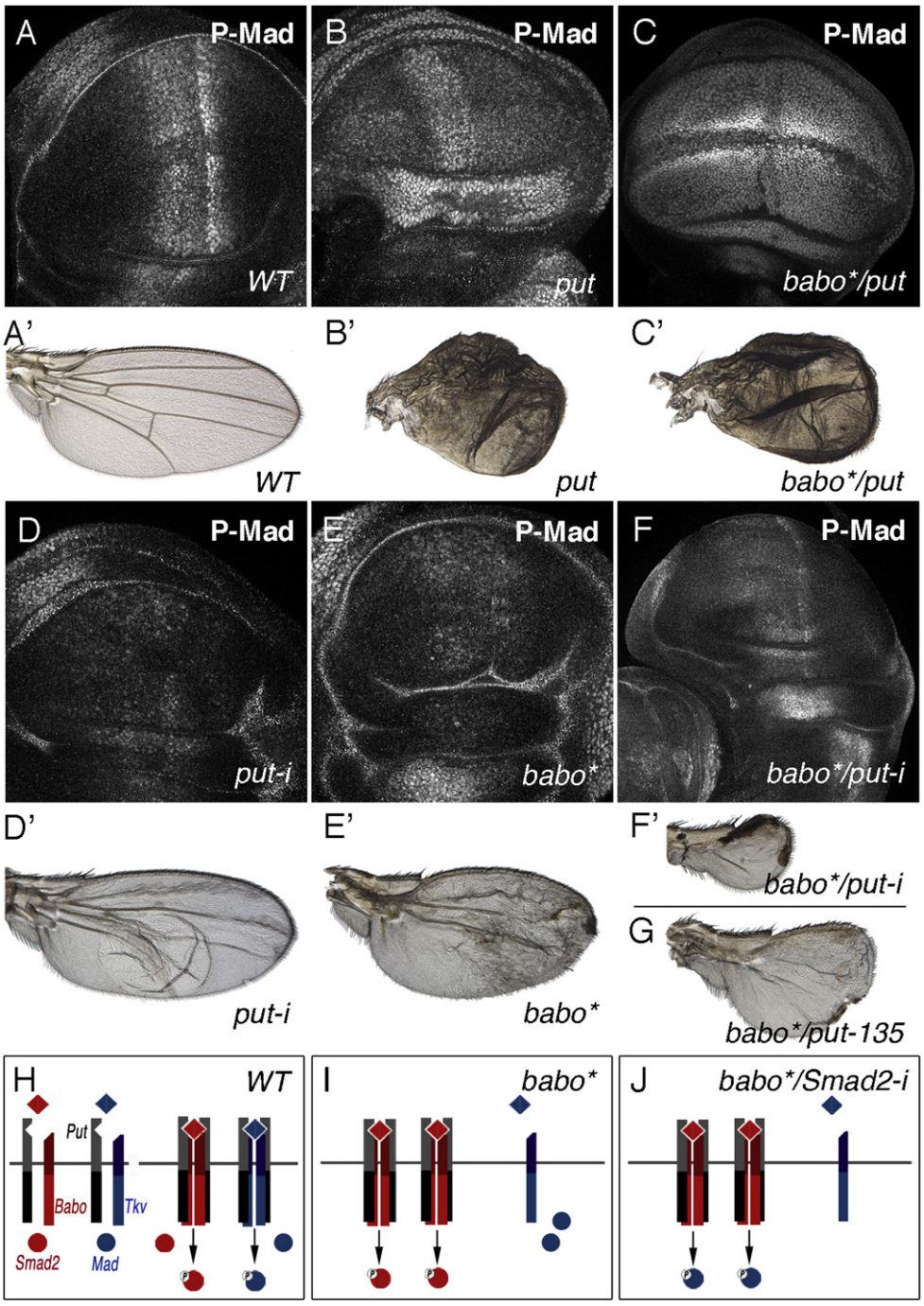

Fig. 9. Punt levels determine the antagonism between BMP and TGFβ signalling. (A–C) Genetic interactions between Babo^{QD} and the over-expression of *punt*. (A) Expression of P-Mad in wild type discs (A), in *nub-Gal4/+*; *UAS-put/+* (*put*; B) and in *nub-Gal4/+*; *UAS-put/UAS-babo^{QD}* (*babo*/put*; C). The over-expression of Put causes ectopic accumulation of P-Mad in the entire wing pouch (B), and this effect is also observed in the Babo^{QD} background (C). (A′–C′) Control (WT, A′), *nub-Gal4/+*; *UAS-put/+* (*put*, B′) and *nub-Gal4/+*; *UAS-put/UAS-babo^{QD}* wings (*babo*/put*; C′). Wings over-expressing Put differentiate extra-vein material and are smaller than normal (B′). This phenotype is not modified by the simultaneous over-expression of Babo^{QD} (C′). (D–F) Reduced accumulation of P-Mad in discs with reduced levels of Put (*nub-Gal4/+*; *UAS-put-i/+*, *put-i* in D), in discs expressing Babo^{QD} (*nub-Gal4/+*; *UAS-babo^{QD}/+*, *babo** in E) and in discs expressing Babo^{QD} in a background of reduced *punt* expression (*nub-Gal4/+*; *UAS-punt-i/UAS-babo^{QD}*, *babo*/put-i* in F). (D′–F′) Expression of RNA interference against *punt* results in a weak "thick veins" phenotype of reduced size and differentiation of thicker than normal veins (*nub-Gal4/+*; *UAS-put-i/+*, *put-i* in D′). The expression of Babo^{QD} in a background of reduced *put* levels results in extreme wing size reduction and loss of veins (*nub-Gal4/+*; *UAS-put-i/UAS-babo^{QD}*, *babo*/put-i* in F′), much stronger than expression of only Babo^{QD} (*nub-Gal4/+ UAS-babo^{QD}/+*, *babo** in E′). (G) The expression of Babo^{QD} in heterozygous *put* mutant background (*nub-Gal4/+*; *UAS-babo^{QD}/punt^{135}*, *babo*/put*-135 in G) results in a stronger wing size reduction and loss of veins than expression of Babo^{QD} in a wild type background (E′). (H–J) Model of BMP-TGFβ cross-interactions in the wing disc. (H) Schematic representation of the type I (Babo and Tkv) and type II receptors (Put), TGFβ and BMP ligands (red and blue squares) and Smad2 and Mad transducers (red and blue circles). Ligand binding causes the assembly of receptor complexes (Babo–Put and Tkv–Put) and phosphorilation of Smad2 and Mad. The activated state of the pathway is shown to the right. (I) Over-expression of Babo^{QD} (babo*) increases Smad2 phosphorylation (P) and, at the same time, reduces the pull of Put available to interact with Tkv, preventing Mad phosphorylation. (J) When the level of Smad2 is low (*babo*/Smad2-i*), Mad can be recruited to Babo^{QD}–Put complexes. This would lead to the observed expansion of Mad phosphorylation. The cell membrane is represented by horizontal grey lines.

size (*nub-Gal4/UAS-babo^{QD}*; Fig. 9E′), but P-Mad is detected at lower than normal levels in the wing disc (Fig. 9E). When Babo^{QD} and Punt are over-expressed in the same domain, the resulting wings are identical to those over-expressing only Put

(*nub-Gal4*/+; *UAS-babo*^{QD}/*UAS-put*; Fig. 9C′), and the expression of P-Mad is also detected in the entire wing blade region of the disc (Fig. 9C). These results indicate that Put over-expression rescues the loss of P-Mad caused by Babo^{QD}. The expression of RNAi against *put* (*put-i*) results in wings that differentiate thicker than normal veins (*nub-Gal4*/+;*UAS-put-i*/+; Fig. 9D′), and the levels of P-Mad accumulation are reduced in the corresponding discs (Fig. 9D). When Babo^{QD} is introduced in this genetic background, the wings are extremely reduced in size and fail to differentiate the veins (*nub-Gal4*/+; *UAS-babo*^{QD}/*UAS-punt-i*; Fig. 9F′). The corresponding wing discs also show a strong reduction in P-Mad expression in the wing blade region (Fig. 9F). A similar enhancement of the wing size reduction and loss of veins caused by Babo^{QD} is observed when this receptor is expressed in *put* heterozygous flies (*nub-Gal4*/+; *UAS-babo*^{QD}/*put*^{135}; Fig. 9G). These results indicate that the loss of veins and the reduction in wing size caused by Babo^{QD} over-expression are extremely sensitive to the levels of Punt expression, being more manifest when *put* expression is reduced.

Discussion

In this work, we have analysed the requirements of TGFβ/Act signalling and its interactions with the related BMP pathway during Drosophila wing development. We find that the knockdown of the four TGFβ candidate ligands (*actβ*, *daw*, *mav* and *myo*), the TGFβ-specific receptor *babo* and its R-Smad effector Smad2 result in wing phenotypes of reduced wing size without affecting the patterning of veins. These smaller wings contain a lower number of cells, suggesting that cell proliferation is reduced in TGFβ mutant conditions. In addition, loss of *babo* and *Smad2* also modified cell size, causing the formation of larger than normal cells. In this manner, our results indicate that the requirement of *babo* for wing growth (Brummel et al., 1999) is autonomous to the wing disc, and show that all members of the pathway participate in this process in the same manner than *babo*. We did not find much effects of Smad2 in the formation of veins, as was reported by Sander et al. (2010). Thus, the phenotypes of extra-veins we observed are very weak compared to those caused by increased Mad signalling, and we think that they may be due to the competition between Mad and Smad2 for Babo that we detected under particular experimental conditions (see below). We also found that hyper-activation of the pathway causes the formation of larger than normal wings, a phenotype opposite to loss of pathway activity. In this case, however, the effects of Babo and Smad2 were different, because activated Babo also causes the differentiation of considerable extra-vein tissue, whereas the expression of phosphomimic Smad2 does not have major effects on the pattern of veins, as also found by Gesualdi and Haerry (2007). In addition, we identify a substantial dose-dependent effect of activated Babo that was not observed with phosphomimic Smad2. Thus, an increase in the level of Babo^{QD} results in strong BMP loss-of-function phenotypes that might be caused by molecular competition among common and specific components of the TGFβ and BMP pathways.

The role of TGFβ signalling in cell proliferation and growth

The cellular and molecular bases of the growth promoting effect of TGFβ signalling are still unknown. It was found that the incorporation of BrdU is not affected in *babo* mutant discs (Brummel et al., 1999), suggesting that Babo does not regulate the progression of the cell cycle. In agreement, we could not detect any effect of *Smad2* loss in the percentage of cells in the G1, S and G2 phases of the cell cycle, suggesting that the pathway does not act primarily in promoting the G1/S or G2/M transitions. We observed that the division rate of *babo* mutant cells is slower than normal, as reflected by the differences in size between *babo* clones and their wild type twins. This effect could be caused by a lengthening of both the G1 and G2 phases of the cell cycle. Contrariwise, a shortening of both G1 and G2 could cause the increase in cell number observed in wings expressing phosphomimic Smad2, where we also found an increase in the fraction of mitotic cells. The changes in wing size we observed are also associated to alterations in cellular size. Thus, *babo* and *Smad2* mutant cells are larger than normal, and cells expressing the activated form of Smad2 (Smad2^{SDVD}) reached a smaller than normal size. It might be that a Babo/Smad2 function regulating cell growth affects the length of the cell cycle. For example, *babo* mutant cells might stay for an extended time between successive mitosis because they increase their cellular mass at a lower rate than normal cells. In this scenario, a key role of TGFβ signalling might be the modulation of other pathways, such as Insulin receptor signalling, that regulate cell growth in the wing disc and also affect cell division (Oldham et al., 2002). We detected some cell death in *babo* mutant discs. However, we thick that the lower number of cells present in *babo* and *Smad2* mutant wings is not related to cell death, as their effects are not modified by preventing cell death.

TGFβ signalling domains in the wing disc and ligand requirements

We found that all four candidates TGFβ ligands are expressed in the wing disc (see also Gesualdi and Haerry, 2007; Parker et al., 2006), and that their expression in this tissue is needed for the wing to reach its normal size. In this respect, our results somehow disagree with the finding that Myo and Mav are not able to promote Smad2 phosphorylation in cell culture experiments (Gesualdi and Haerry, 2007). Also, the expression of *actβ* and *daw* was not detected in wing discs (Gesualdi and Haerry, 2007), which implicated that Babo and Smad2 in the imaginal discs was activated by ligands coming from the central nervous system, where their expression is certainly more robust. In this manner, it was suggested that TGFβ ligands worked in imaginal cells acting as paracrine signals (Gesualdi and Haerry, 2007). In our hands, all ligands are expressed in the discs, although the level of *actβ* expression is indeed very low (see Fig. 6 and Supplementary Fig. 6). Furthermore, the expression of the corresponding RNA interference in the wing blade is sufficient to reduce the size of the wing. The phenotypes we observed upon a reduction in *actβ*, *daw*, *mav* and *myo* in the wing were always weaker than those caused by loss of *babo* or *Smad2*. This is in part due to the incomplete knockdown produced by RNAi expression, as detected by real-time RT-PCR and in situ hybridisation (Supplementary Fig. 6). Furthermore, different UAS insertions of the same RNAi often result in quantitatively different phenotypes (Supplementary Fig. 5), indicating that with this approach we are only generating hypomorphic conditions of the targeted gene. We found synergistic effects when the expression of more than one ligand was reduced simultaneously in the wing blade. However, we cannot distinguish between the four ligands acting cooperatively or independently, due to the hypomorphic nature of the RNAi approach. For the same reason, we cannot exclude a paracrine contribution of the ligands, although our results suggest that the ligands act additively to promote Smad2 phosphorylation, and that the source of these ligands are the imaginal cells.

In contrast to BMP signalling, which activation is spatially restricted, the activation of Babo, as visualised by the accumulation of phosphorylated Smad2, occurs in all imaginal wing cells. We detected lower levels of P-Smad2 around the dorso-ventral boundary in late third instar wing discs, and this reduction is

correlated with lower levels of *Smad2* expression (see Fig. 6A). In this manner, it seems that the expression level of the *Smad*2 gene, more than a differential activation of the receptor, is responsible of this local modulation in Smad2 phosphorylation.

Cross-interactions between the TGFβ and BMP pathways in the wing disc

The analysis of cross-interactions between the TGFβ and BMP pathways is complicated because both pathways share several common elements, including the type II receptor Put and the co-Smad Med. Our results confirm that a constitutive active form of Babo is capable to activate Mad (Gesualdi and Haerry, 2007; Peterson et al., 2012). As recently reported, this effect is only observed in the wing disc when *Smad*2 expression is reduced (Peterson et al., 2012). We emphasise that neither over-expression of the normal version of Babo nor the reduction in the levels of *babo* expression affect the accumulation of P-Mad in this tissue. In this manner, it is unlikely that Babo had physiological effects on Mad phosphorylation during the development of the wing disc. The effects of changing *Smad*2 levels of expression are more complex, because the reduction of *Smad*2 in a particular spatial domain of the wing disc causes an expansion of lateral regions of the wing blade, as was first observed by Sander et al. (2010). In these discs, we observed both a reduction in the size of the wing pouch, confirming the requirement of Smad2 to promote growth, and an increase in the size of the lateral regions. This last effect is correlated with the loss of *brk* expression, and because *brk* is repressed by Dpp/BMP signalling (Affolter and Basler, 2007), its loss of expression upon a reduction of *Smad*2 levels suggest that Smad2 can play a role in preventing inappropriate Dpp/BMP signalling in the lateral regions of the wing disc. Unexpectedly, we did not find ectopic P-Mad associated to the regions where *brk* expression is reduced, which we interpret as a failure to detect the low levels of P-Mad accumulation that might be sufficient to prevent *brk* expression.

The expression of activated Babo causes a severe reduction in the accumulation of phosphorylated Mad in the presence of Smad2. This effect leads to a loss of BMP function phenotype in the wing that is strongly dependent in the level of *put* expression. Therefore, we suggest that activated Babo expressed at higher than normal levels increases the recruitment of the type II receptor Put, resulting in a concomitant reduction in the fraction of Put complexed with the BMP receptor Tkv (Fig. 9I). In the presence of Smad2, the accessibility of Mad to the dominant Babo/Put heterodimers is prevented, and the reduction in Tkv/Put complexes results in the loss of P-Mad (Fig. 9I). When Smad2 is not available, Mad can be recruited to Babo/Put complexes, favouring the accumulation of P-Mad (Fig. 9J). Similar interactions between activated Babo, Smad2 and Mad have been recently described by biochemical and genetic experiments (Peterson et al., 2012). These authors also detected a possible role for the Smad2 antagonism of Mad phosphorylation in particular developmental systems, such as in cells of the fat body and gut (Peterson et al., 2012).

Interactions between the TGFβ and BMP pathways are complex and context-dependent, and in many instances BMP and TGFβ display opposing cellular outcomes. The divergent responses to these pathways rely in part on the different set of target genes regulated by them (Kowanetz et al., 2004; Yang et al., 2004), but also in the differential regulation of common target genes. For example, TGFβ represses and BMP signalling activates the expression of the Id genes Id2 and Id3 in mammary epithelial cells (Kowanetz et al., 2004). Because these genes play a prominent role regulating the choice between cell proliferation and differentiation, the correct balance between BMP and TGFβ signalling is critical to regulate cell behaviour, and this coordination is likely of general importance during normal development and in situations where miss-regulation of some component of the pathways leads to diseases. Our results suggest that miss-regulation in the expression of receptors and Smad proteins could lead to strong changes in P-Smad2 and P-Mad accumulation in a given cell, resulting in severe alterations in BMP/TGFβ regulated cell behaviours. These alterations might be of special importance in organisms where more combinations between receptors, receptor isoforms and ligands occur in different cell types (Venkatasubbarao et al., 2000).

Acknowledgements

We are very grateful to Ana López-Varea, Verónica Flores and Elena de Celis for their skilful technical help, María F. Organista for sharing unpublished results and Alberto Mudarra from the Genomic service of the CBMSO for his help with qRT-PCRs. We thank the Hybridome bank at Iowa University, NIG in Japan, VDCR in Vienna, Bloomington Stock Center, Gines Morata, Peter Ten Dike, Theodor Haerry, Konrad Basler, and other colleagues for providing the tools necessary for this work. Antonio Baonza, Carlos Estella, Antonio Montes and Cristina Molnar are also acknowledged for criticism that greatly improved the manuscript.

Appendix A. Supporting information

Supplementary data associated with this article can be found in the online version at http://dx.doi.org/10.1016/j.ydbio.2013.02.004.

References

Affolter, M., Nellen, D., Nussbaumer, U., Basler, K., 1994. Multiple requirements for the receptor serine/threonine kinase thick veins reveal novel functions of TGF beta homologs during Drosophila embryogenesis. Development 120, 3105–3117.

Affolter, M., Basler, K., 2007. The Decapentaplegic morphogen gradient: from pattern formation to growth regulation. Nat. Rev. Genet. 8, 663–674.

Brummel, T., Abdollah, S., Haerry, T.E., Shimell, M.J., Merriam, J., Raftery, L., Wrana, J.L., O'Connor, M.B., 1999. The Drosophila activin receptor baboon signals through dSmad2 and controls cell proliferation but not patterning during larval development. Genes Dev. 13, 98–111.

Burke, R., Basler, K., 1996. Dpp receptors are autonomously required for cell proliferation in the entire developing Drosophila wing. Development 122, 2261–2269.

Campbell, G., Tomlinson, A., 1999. Transducing the Dpp morphogen gradient in the wing of Drosophila: regulation of Dpp targets by brinker. Cell 96, 553–562.

Cruz, C., Glavic, A., Casado, M., de Celis, J.F., 2009. A gain-of-function screen identifying genes required for growth and pattern formation of the *Drosophila melanogaster* wing. Genetics 183, 1005–1026.

Das, P., Inoue, H., Baker, J.C., Beppu, H., Kawabata, M., Harland, R.M., Miyazono, K., Padgett, R.W., 1999. Drosophila dSmad2 and Atr-I transmit activin/TGFbeta signals. Genes Cells 4, 123–134.

de Celis, J.F., 1997. Expression and function of decapentaplegic and thick veins during the differentiation of the veins in the Drosophila wing. Development 124, 1007–1018.

de Celis, J.F., Barrio, R., Kafatos, F.C., 1996. A gene complex acting downstream of dpp in Drosophila wing morphogenesis. Nature 381, 421–424.

Drysdale, R., 2008. FlyBase: a database for the Drosophila research community. Methods Mol. Biol. 420, 45–59.

Estella, C., McKay, D.J., Mann, R.S., 2008. Molecular integration of *wingless*, *decapentaplegic* and autoregulatory inputs into Distal-less during Drosophila leg development. Dev. Cell 14, 86–96.

Gesualdi, S.C., Haerry, T.E., 2007. Distinct signaling of Drosophila Activin/TGF-beta family members. Fly (Austin) 1, 212–221.

Gibson, M.C., Perrimon, N., 2005. Extrusion and death of DPP/BMP-compromised epithelial cells in the developing Drosophila wing. Science 307, 1785–1789.

Huang, F., Chen, Y.-G., 2012. Regulation of TGF-β receptor activity. Cell Biosci. 2, 1–9.

Jazwinska, A., Kirov, N., Wieschaus, E., Roth, S., Rushlow, C., 1999. The Drosophila gene brinker reveals a novel mechanism of Dpp target gene regulation. Cell 96, 563–573.
Kowanetz, M., Valcourt, U., Bergstrom, R., Heldin, C.H., Moustakas, A., 2004. Id2 and Id3 define the potency of cell proliferation and differentiation responses to transforming growth factor beta and bone morphogenetic protein. Mol. Cell Biol. 24, 4241–4254.
Martin, F.A., Perez-Garijo, A., Moreno, E., Morata, G., 2004. The brinker gradient controls wing growth in Drosophila. Development 131, 4921–4930.
Massague, J., Blain, S.W., Lo, R.S., 2000. TGFbeta signaling in growth control, cancer, and heritable disorders. Cell 103, 295–309.
Massague, J., Seoane, J., Wotton, D., 2005. Smad transcription factors. Genes Dev. 19, 2783–2810.
Massague, J., Wotton, D., 2000. Transcriptional control by the TGF-beta/Smad signaling system. EMBO J. 19, 1745–1754.
Minami, M., Kinoshita, N., Kamoshida, Y., Tanimoto, H., Tabata, T., 1999. brinker is a target of Dpp in Drosophila that negatively regulates Dpp-dependent genes. Nature 398, 242–246.
Molnar, C., Ruiz-Gómez, A., Martín, M., Rojo-Berciano, S., Mayor, F., de Celis, J.F., 2011. Role of the Drosophila non-visual β-arrestin kurtz in hedgehog signalling. PLoS Genet 7 (3), e1001335.
Nellen, D., Burke, R., Struhl, G., Basler, K., 1996. Direct and long-range action of a DPP morphogen gradient. Cell 85, 357–368.
O'Brochta, D.A., Bryant, P.J., 1985. A zone of non-proliferating cells at a lineage restriction boundary in Drosophila. Nature 313, 138–141.
Oldham, S., Stocker, H., Laffargue, M., Wittwer, F., Wymann, M., Hafen, E., 2002. The Drosophila insulin/IGF receptor controls growth and size by modulating PtdInsP(3) levels. Development 129, 4103–4109.
Parker, L., Ellis, J.E., Nguyen, M.Q., Arora, K., 2006. The divergent TGF-beta ligand Dawdle utilizes an activin pathway to influence axon guidance in Drosophila. Development 133, 4981–4991.
Parker, L., Stathakis, D.G., Arora, K., 2004. Regulation of BMP and activin signaling in Drosophila. Prog. Mol. Subcell. biol. 34, 73–101.
Persson, U., Izumi, H., Souchelnytskyi, S., Itoh, S., Grimsby, S., Engstrom, U., Heldin, C.H., Funa, K., ten Dijke, P., 1998. The L45 loop in type I receptors for TGF-beta family members is a critical determinant in specifying Smad isoform activation. FEBS Lett. 434, 83–87.
Peterson, A.J., Jensen, P.A., Shimell, M., Stefancsik, R., Wijayatonge, R., Herder, R., Raftery, L., O'Connor, M.B., 2012. R-Smad competition controls Activin receptor output in Drosophila. PLOS One 7, e36548.
Posakony, L.G., Raftery, L.A., Gelbart, W.M., 1990. Wing formation in Drosophila melanogaster requires decapentaplegic gene function along the anterior–posterior compartment boundary. Mech. Dev. 33, 69–82.
Raftery, L.A., Sutherland, D.J., 1999. TGF-beta family signal transduction in Drosophila development: from Mad to Smads. Dev. Biol. 210, 251–268.
Sander, V., Eivers, E., Choi, R.H., De Robertis, E.M., 2010. Drosophila Smad2 opposes Mad signaling during wing vein development. PLoS One 5, e10383.
Sanicola, M., Sekelsky, J., Elson, S., Gelbart, W.M., 1995. Drawing a stripe in Drosophila imaginal disks: negative regulation of decapentaplegic and patched expression by engrailed. Genetics 139, 745–756.
Schmierer, B., Hill, C.S., 2007. TGFβ-SMAD signal transduction: molecular specificity and functional flexibility. Nat. Rev. Mol. Cell Biol. 8, 970–982.
Schwank, G., Restrepo, S., Basler, K., 2008. Growth regulation by Dpp: an essential role for Brinker and a non-essential role for graded signaling levels. Development 135, 4003–4013.
Teleman, A.A., Cohen, S.M., 2000. Dpp gradient formation in the Drosophila wing imaginal disc. Cell 103, 971–980.
Ting, C.Y., Herman, T., Yonekura, S., Gao, S., Wang, J., Serpe, M., O'Connor, M.B., Zipursky, S.L., Lee, C.H., 2007. Tiling of r7 axons in the Drosophila visual system is mediated both by transduction of an activin signal to the nucleus and by mutual repulsion. Neuron 56, 793–806.
Venkatasubbarao, K., Ahmed, M.M., Mohiuddin, M., Swiderski, C., Lee, E., Gower, W.R., Jr. Salhab, K.F., McGrath, P., Strodel, W., Freeman, J.W., 2000. Differential expression of transforming growth factor-β receptors in human pancreatic adenocarcinoma. Anticancer Res. 20, 43–51.
Wu, M.Y., Hill, C.S., 2009. Tgf-beta superfamily signaling in embryonic development and homeostasis. Dev. Cell 16, 329–343.
Yang, M., Nelson, D., Funakoshi, Y., Padgett, R.W., 2004. Genome-wide microarray analysis of TGFbeta signaling in the Drosophila brain. BMC Dev. Biol. 4, 14.
Zheng, X., Wang, J., Haerry, T.E., Wu, A.Y., Martin, J., O'Connor, M.B., Lee, C.H., Lee, T., 2003. TGF-beta signaling activates steroid hormone receptor expression during neuronal remodeling in the Drosophila brain. Cell 112, 303–315.
Zheng, X., Zugates, C.T., Lu, Z., Shi, L., Bai, J.M., Lee, T., 2006. Baboon/dSmad2 TGF-beta signaling is required during late larval stage for development of adult-specific neurons. EMBO J. 25, 615–627.
Zhu, C.C., Boone, J.Q., Jensen, P.A., Hanna, S., Podemski, L., Locke, J., Doe, C.Q., O'Connor, M.B., 2008. Drosophila Activin- and the Activin-like product Dawdle function redundantly to regulate proliferation in the larval brain. Development 135, 513–521.